EUR 3883 e

EUROPEAN ATOMIC ENERGY COMMUNITY — EURATOM

CALCULATING THE CRITICAL VELOCITIES OF A "CHOPPER"

by

M. BIGGIO

1968

Joint Nuclear Research Center
Ispra Establishment — Italy

General Studies and Radioactive Engineering

LEGAL NOTICE

This report is on sale at the addresses listed on cover page 4

at the price of FF 8.50	FB 85.—	DM 6.80	Lit. 1060	Fl. 6.20

When ordering, please quote the EUR number and the title, which are indicated on the cover of each report.

Printed by Van Muysewinkel
Brussels, April 1968

EUR 3883 e

CALCULATING THE CRITICAL VELOCITIES OF A "CHOPPER" by M. BIGGIO

European Atomic Energy Community - EURATOM
Joint Nuclear Research Center - Ispra Establishment (Italy)
General Studies and Radioactive Engineering
Brussels, April 1968 - 62 Pages - 11 Figures - FB 85

This report deals with the calculation of the critical velocities—those due to torsional, flexional and precession movements—of a "chopper".

The purpose of the report is to show the process by which these speeds are calculated for an unusual mechanical system.

The approach is not new in itself, being that traditionally used in mechanical engineering. We believe, however, that a demonstration of the working of the problem right through to the numerical value will help to overcome the difficulties which would inevitably be encountered by anyone working solely on the basis of the general principles which we took as a starting point.

EUR 3883 e

CALCULATING THE CRITICAL VELOCITIES OF A "CHOPPER" by M. BIGGIO

European Atomic Energy Community - EURATOM
Joint Nuclear Research Center - Ispra Establishment (Italy)
General Studies and Radioactive Engineering
Brussels, April 1968 - 62 Pages - 11 Figures - FB 85

This report deals with the calculation of the critical velocities—those due to torsional, flexional and precession movements—of a "chopper".

The purpose of the report is to show the process by which these speeds are calculated for an unusual mechanical system.

The approach is not new in itself, being that traditionally used in mechanical engineering. We believe, however, that a demonstration of the working of the problem right through to the numerical value will help to overcome the difficulties which would inevitably be encountered by anyone working solely on the basis of the general principles which we took as a starting point.

EUR 3883 e

EUROPEAN ATOMIC ENERGY COMMUNITY — EURATOM

CALCULATING THE CRITICAL VELOCITIES OF A "CHOPPER"

by

M. BIGGIO

1968

Joint Nuclear Research Center
Ispra Establishment — Italy

General Studies and Radioactive Engineering

Summary

This report deals with the calculation of the critical velocities—those due to torsional, flexional and precession movements—of a "chopper".

The purpose of the report is to show the process by which these speeds are calculated for an unusual mechanical system.

The approach is not new in itself, being that traditionally used in mechanical engineering. We believe, however, that a demonstration of the working of the problem right through to the numerical value will help to overcome the difficulties which would inevitably be encountered by anyone working solely on the basis of the general principles which we took as a starting point.

KEYWORDS

VELOCITY
ROTATION
VIBRATION
TORSION
FAILURES
MACHINE PARTS
BEARINGS
PRECESSION
STRESSES
TENSILE PROPERTIES
MATERIALS TESTING
CYLINDERS
CHOPPERS

CONTENTS

INTRODUCTION

The importance of the study of torsional, flexional and precessional vibrations in rotating systems is recognized by constructors and users who for some time have had to suffer the consequences of these vibrations, which culminate in shaft fractures at critical velocities.

When designing a rotating system, fundamental importance must be given to the calculation of the critical torsional, flexional and precessional velocities, in order to provide the system with working velocities involving no dangerous oscillations of such a kind as would be liable sooner or later to cause failure of the shafts.

The rotating system under consideration is of the "suspended" type, that is to say vertical, attached at the top and free at the bottom. As fig. 1 shows, it consists, very simply, of a vertical shaft made up of various lengths of different diameter, with the electric motor at its upper and the chopper-rotor at its lower end.

Our system differs from the rotating systems usually employed in mechanical engineering, both in type and in the length of small-diameter shafting, 3 mm in diameter. This configuration has a highly important purpose, namely to allow the chopper-rotor to find its own position of dynamic equilibrium, thus avoiding the concentration of heavy loads on the ball-bearings which would very soon fail under such conditions.

For obvious reasons of clarity, the present calculation has been broken down into 4 consecutive parts as follows:

- Calculation of the critical torsional velocities
- Calculation of the critical flexional velocities
- Calculation of the critical precession velocities
- Conclusions.

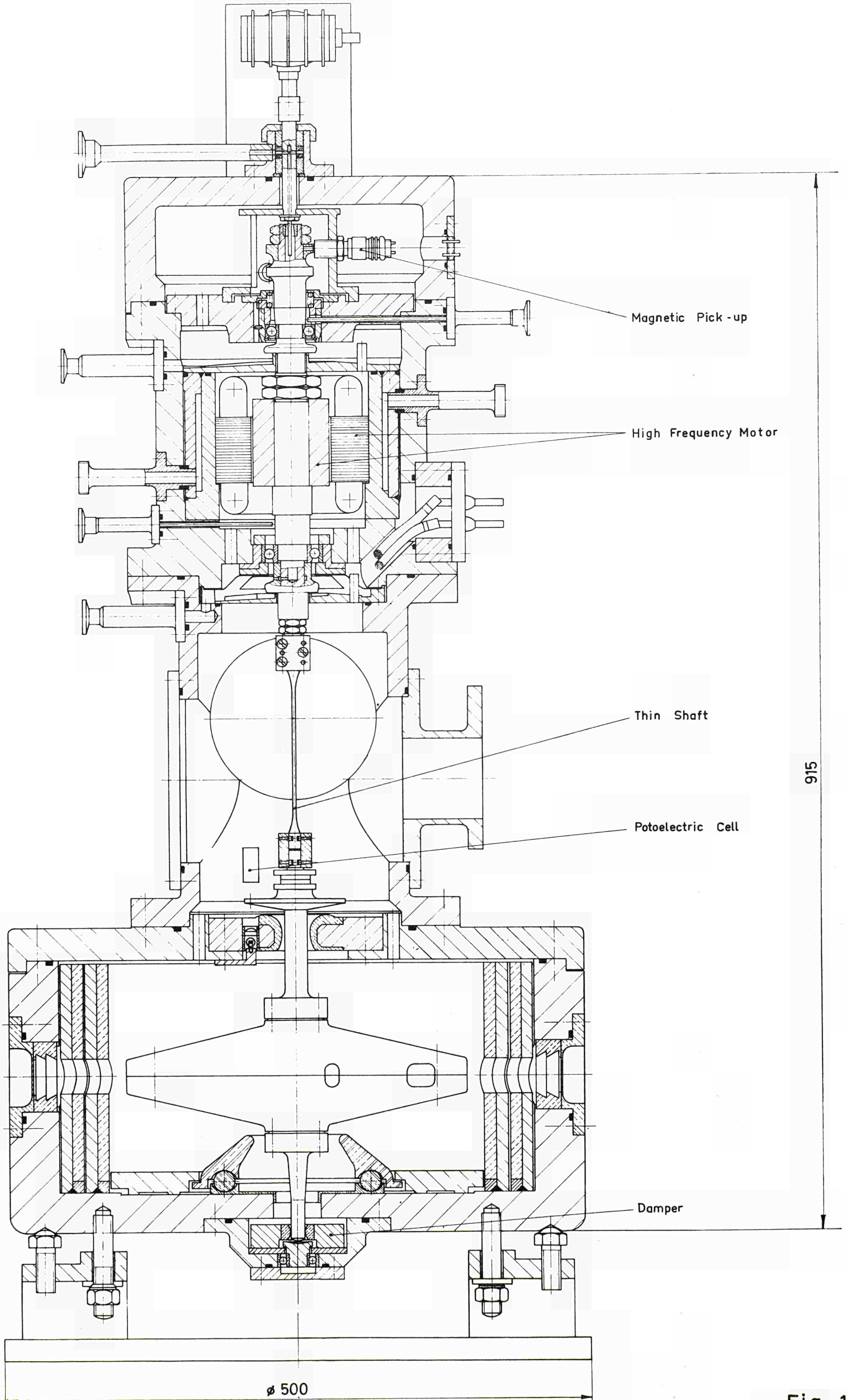
Magnetic Pick-up
High Frequency Motor
Thin Shaft
Potoelectric Cell
Damper
915
ø 500

Fig. 1

A fifth section has been added, which contains the experimental results. Also, as we are dealing with a particular system, in section II the chief effects (gyroscopic and traction) which effect the flexional vibrations have been introduced one by one into the calculation so that their influence on the critical flexional velocities may be observed. In Appendix I and II methods are indicated which allow to introduce also the effects of rotatory inertia and of transverse shear into the calculation of the critical velocities of bending.

Although the calculation method relates here to the system depicted in Fig. 1, it is general and can be applied to any rotating device.

1. CALCULATION OF THE CRITICAL TORSIONAL VELOCITIES

It has now become the general practice to calculate the critical torsional velocities on suitable "reduced" systems which are thought of as having attached to them, at suitable intervals, imaginary flywheels having an appropriate moment of inertia but assumed to be without thickness, that is to say, concentrated along their plane of attachment to the line of the shaft. (Ref. 1).

In every case, the reduced system will have to be representative of the actual vibrating system and equivalent to it as regards torsional behaviour; it is therefore necessary, at the outset, to define the dynamic characteristics by means of a "mass- and length-reducing" operation, this being carried out as follows:

1.1 <u>Reduction of masses</u>

The cases commonly encountered in practice concern masses in reciprocating motion, in rotary motion, and in combined rotary and reciprocating motion. As far as the torsional vibrations are concerned, these masses may be considered simply in two groups:

- masses in reciprocating motion, and
- masses in rotary motion.

In both cases, the real masses are replaced by an ideal flywheel having an equivalent moment of inertia, which is obtained by equating the kinetic energies in play.

In the case of masses in reciprocating motion, given that

m_a = mass in reciprocating motion
V = instantaneous velocity of the mass in reciprocating motion
Ω = angular velocity of rotation of the shaft
Y = equivalent moment of inertia

we have

$$1/2\ Y\ \Omega^2 = 1/2\ m_a\ V^2$$

which gives

$$Y = m_a (V/\Omega)^2 \qquad (1)$$

In the case of masses in rotary motion, given that

Y_1 = moment of inertia of the mass in rotary motion
Ω_1 = angular velocity of rotation of the shaft carrying the mass whose moment of inertia is Y_1
n_1 = number of revolutions of the shaft carrying the mass of moment Y_1
Ω = angular velocity of rotation of the driving shaft
Y = equivalent moment of inertia
n = number of revolutions of the driving shaft

we have

$$1/2\ Y\ \Omega^2 = 1/2\ Y_1\ \Omega_1^2$$

from which

$$Y = Y_1\,(\Omega_1/\Omega)^2 = Y_1\,(n_1/n)^2 \tag{2}$$

if $\Omega = \Omega_1$, i.e. if the mass is carried on the driving shaft we get

$$Y = Y_1 \tag{2'}$$

i.e. it is sufficient to replace each real mass by an ideal flywheel without thickness, having a moment of inertia equal to that of the given mass.

1.2 Reduction of lengths

For the reduction of lengths it is customary to take a constant diameter as basic diameter for all calculations (Ref. 1) 2)).

All the component sections of the shafting of the system in question will therefore be reduced to sections of this diameter with lengths varied so as to correspond elastically to the real lengths.

For this it is sufficient to equate the torsional rigidities.

Let us recall that the torsional rigidity (or elastic constant) for a cylindrical shaft of diameter D and length l is defined as having the value

$$K = \frac{G\ J_p}{l} = \frac{G\ \frac{\pi}{32}\ D^4}{l}$$

where G is the tangential elastic modulus.

Thus, if

l_v = true length of the generic section making up the shaft

D_v = true diameter of the generic section making up the shaft

l_r = reduced length of the said section

D_r = constant basic diameter

for every section we shall have

$$\frac{G \frac{\pi}{32} D_r^4}{l_r} = \frac{G \frac{\pi}{32} D_v^4}{l_v}$$

whence

$$l_r = l_v (D_r/D_v)^4 \qquad (3)$$

For a hollow cylindrical shaft whose external and internal diameters are respectively D_v and d_v, we have

$$\frac{G \frac{\pi}{32} D_r^4}{l_r} = \frac{G \frac{\pi}{32} (D_v^4 - d_v^4)}{l_v}$$

whence

$$l_r = l_v \left(\frac{D_r^4}{D_v^4 - d_v^4}\right) \qquad (3')$$

The reduction of conical sections, joints, etc. is effected by means of special tables or formulae to be found in textbooks on the subject.

1.3 Calculation of the ideal system

On the basic of the foregoing, the system under study may be reduced to a certain number of flywheels interconnected by cylindrical shaft sections of constant diameter; where calculation of the critical velocities is concerned, reference is always made to the ideal system thus obtained, disregarding the actual system which it represents.

1.3.1 Calculation of the proper frequencies

To calculate the proper frequencies of the ideal elastic system obtained as shown above, we follow the standard method consisting in equating the moment of the elastic reactions, which is determined in each shaft section in relation to the maximum amplitude of the oscillation, with the aggregate inertia couple which is applied at the end of the section.

Thus calling:

- Y_m the moments of inertia of the Z flywheels;
- θ_m the respective amplitudes of vibration (m goės from 1 to Z);
- K_m the elastic constants of the interposed shaft sections (m goes from 1 to (Z - 1));
- Ω a natural oscillation of the system.

the moment of the elastic reactions in the i^{th} section is

$$M_i = K_i \left(\theta_{i+1} - \theta_i\right)$$

and the aggregate inertia couple is

$$C_i = \sum_{m=1}^{i} Y_m \left(\frac{d^2 \theta}{d t^2}\right)$$

Bearing in mind that the elastic vibrations are simple sinusoidals

$$\theta = \theta_m \sin \Omega t$$

whence

$$\frac{d^2 \theta}{d t^2} = - \Omega^2 \theta_m \sin \Omega t$$

The maximum amplitude of oscillation is given by $\sin \Omega\, t = 1$, that is, by

$$\left(\frac{d^2\,\theta}{d\,t^2}\right)_{max} = -\,\Omega^2\,\theta_m$$

It follows therefore that

$$C_i = -\sum_{m=1}^{i} Y_m\,\Omega^2\,\theta_m$$

and from the foregoing

$$\sum_{m=1}^{i} Y_m\,\Omega^2\,\theta_m = K_i(\theta_i - \theta_{i+1}) \tag{4}$$

This formula applied below the Z^{th} flywheel becomes

$$\sum_{m=1}^{i} Y_m\,\Omega^2\,\theta_m = 0 \tag{4'}$$

The value θ_{i+1} of each mass is related to the preceding value θ_i by the following equation:

$$\theta_{i+1} = \theta_i - \frac{\sum_{m=1}^{i} Y_m\,\Omega^2\,\theta_m}{K_i} \tag{5}$$

where

$$K_i = \frac{G\,J_p}{l_i}$$

is the torsional rigidity of the i^{th} section of length l_i of the ideal system with J_p constant, given that in such a system all the sections are of the same diameter.

All the values of Ω which satisfy equation (4') are torsional proper frequencies of the system.

In general it is easier to carry out this calculation indirectly. The amplitude of vibration of the first mass of the system is therefore taken to be equal to 1 radian and a frequency value at which to carry out the trial is chosen. Having established this, by applying equations (4') and (5) it will be possible to calculate successively the amplitude of vibration of each mass and at the same time the torque due to inertia, applied to the sections linking up the said masses.

The frequency adopted in the trial will coincide with one of the actual frequencies of the system whenever equation (4) can be satisfied; that is to say, when below the last mass the torque due to vibration is equal to zero.

The procedure by trial described here, which is usually preferred to the direct determination of the values of Ω by means of algebraic solution of (4'), is made possible by knowing the form of the "remainder function":

$$f(\Omega) = \sum_{m=1}^{i} Y_m \Omega^2 \theta_m$$

As we know, this always follows the pattern shown in Fig. 2 and cancels itself out at the proper frequency values of Ω, i.e. at as many points as there are possible modes of vibration of the system. From the sign assumed by the remainder for the various trial values of Ω it is possible to obtain a useful indication as to whether the value of Ω should be increased or reduced for the next trial.

The remarkably convenient method of calculation explained above is universally known as the HOLZER (or LEWIS) TABULATING METHOD.

The calculation described above can be programmed for a computer, all natural frequencies of the system under consideration are then obtained.

As we have shown, the calculation of the natural frequencies of the system, indicated in Fig. 1 and simplified for purposes of calculation as shown in Fig. 3a, proves particularly simple because it represents the case of a line of shafting connecting two flywheels.

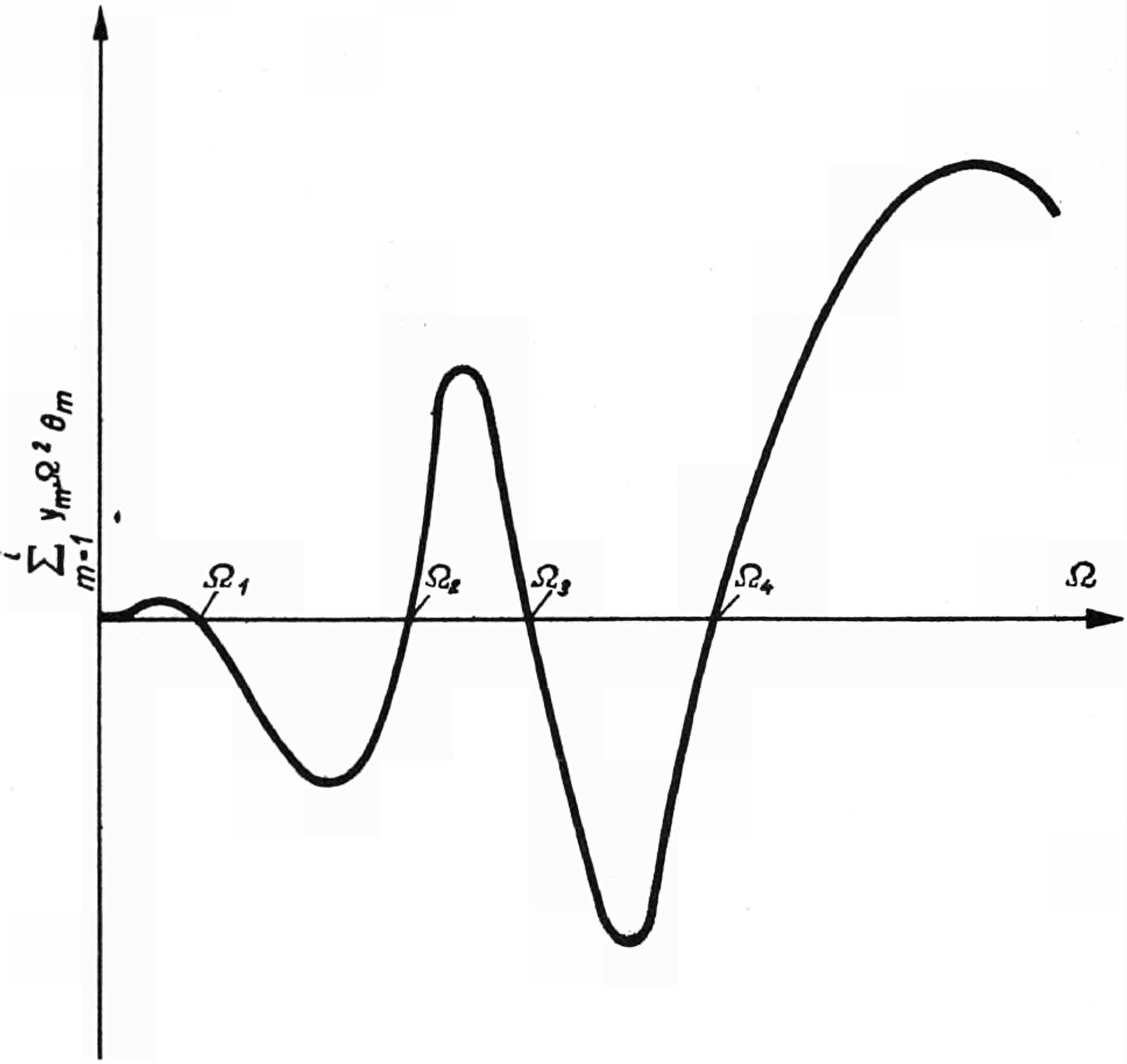

Fig. 2

C.C.R.
ISPRA

EURATOM

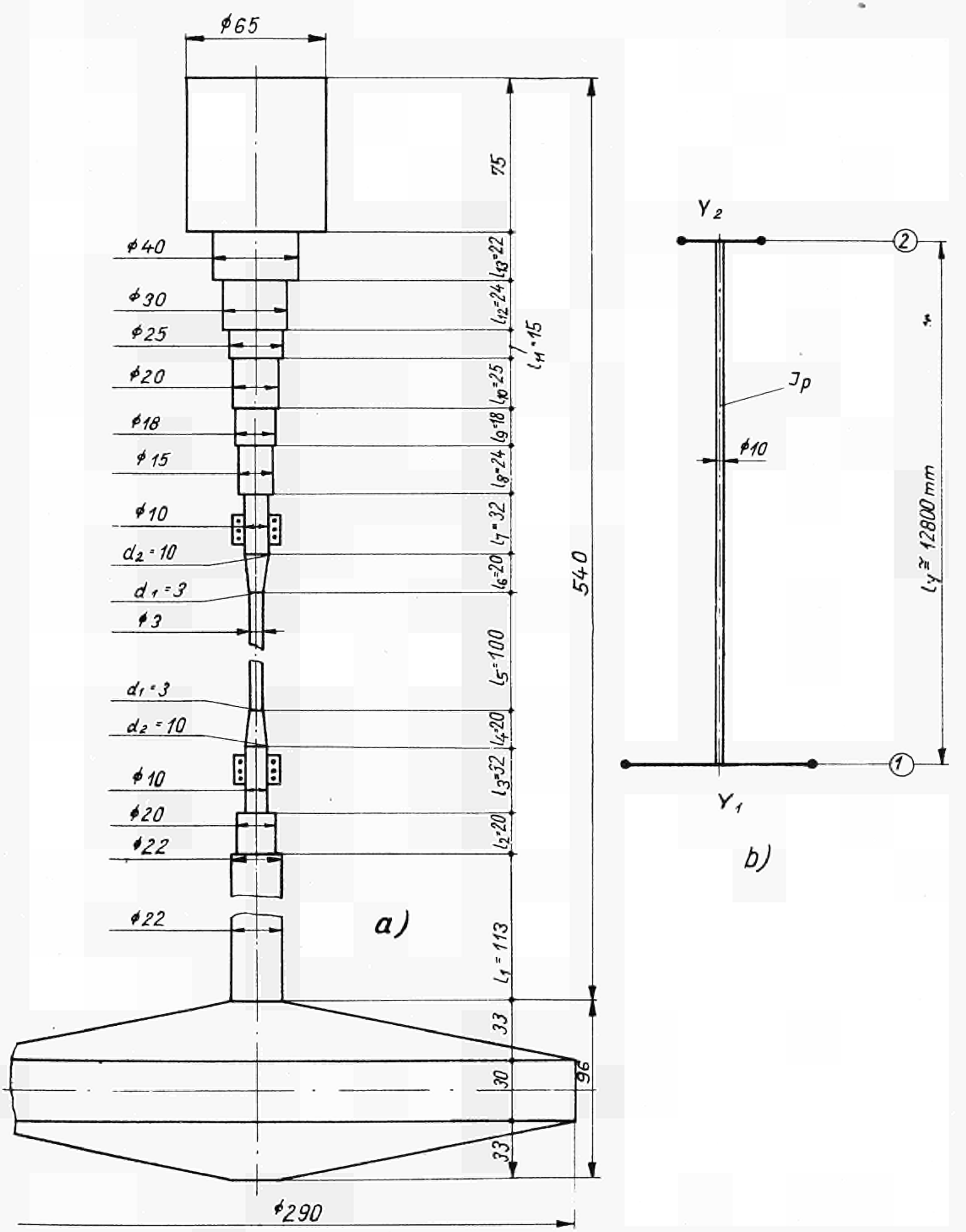

Fig. 3

7.10.63/

In such cases equation (4) gives, for the shaft section connecting the two flywheels:

$$Y_1 \ \Omega^2 \ \theta_1 = K_1 \ (\theta_1 - \theta_2)$$

where

$$K_1 = \frac{G \ J_p}{l_r}$$

is the torsional rigidity of the reduced system (see Fig. 3b).

From this we obtain

$$\frac{\theta_2}{\theta_1} = 1 - \frac{Y_1}{K_1} \Omega^2 \qquad (6)$$

On the other hand, equation (4), when applied below the second flywheel, becomes

$$Y_1 \ \Omega^2 \ \theta_1 + Y_2 \ \Omega^2 \ \theta_2 = 0$$

Dividing by θ_1, we get

$$Y_1 \ \Omega^2 + Y_2 \ \Omega^2 \ \frac{\theta_2}{\theta_1} = 0$$

Substituting for θ_2/θ_1, the value given by equation (6), we obtain:

$$\frac{Y_1 \ Y_2}{K_1} \Omega^4 - \Omega^2 \ (Y_1 + Y_2) = 0$$

whence

$$\Omega = \pm \sqrt{\frac{K_1 \ (Y_1 + Y_2)}{Y_1 Y_2}} = \pm \sqrt{\frac{G \ J_p (Y_1 + Y_2)}{Y_1 \ Y_2 \ l_r}} \qquad (7)$$

This tells us that our system has only one natural frequency which we proceed to calculate (the double sign indicates that the flywheels can revolve in both directions).

With reference to the system shown in Fig. 3a, if we reduce the lengths to an ideal diameter of 10 mm as described in section 1.2 and allow for the correcting factors (1) in respect of conical sections, joints and cross-sectional variations in cylindrical sections, we get:

total reduced length: $L_y \simeq 1{,}280$ cm

Our system is thus transformed, for the purpose of calculating the torsional vibrations, into the equivalent ideal system represented in Fig. 3b, in which

- moment of inertia of mass (1) Y_1 = 2.81 kgcm sec^2
- moment of inertia of mass (2) Y_2 = 0.0106 kgcm sec^2
- polar moment of inertia of reduced shaft J_p = 0.098 cm^4
- tangential elasticity modulus G = 850,000 kg/cm^2

Substituting these values in equation (7), we find

$$\Omega = 78.5 \text{ rad/sec.}$$

whence the only natural frequency of the system:

$$f = \frac{\Omega \times 60}{2\pi} = 750 \text{ /min}$$

It may be objected that in calculating the system in question, the actual mass of the shaft connecting the two flywheels has not been taken into account.

It can be demonstrated that in order to take account of the mass of the shaft it is sufficient to add to the mass moment of inertia of the nearest flywheel 1/3 of the moment of inertia of the shaft which goes from the said flywheel to the nearest node. As may be verified, the latter moment of inertia is very small compared with Y_1 and Y_2 and is therefore negligible.

1.3.2 Determination of the critical torsional velocities

All velocities of the system under consideration which satisfy the relation

$$Fe = f = 750/\mathrm{min}$$

are critical torsional velocities.
Fe is the frequency of excitation of the system due to the electrical driving motor. This is a special high frequency synchronous motor with one pair of poles. It is started asynchronously and synchronized by manual frequency regulation at about 5000 r.p.m.

It is known (2) that for a three-phase asynchronous motor, fed with a frequency F(Hz), the frequency of mechanical excitation is

$$Fe = 2(N_s - N)p$$

where:

N_s [rpm] = velocity of the revolving magnetic flux = 60 F/p

N [rpm] = number of revolutions of the motor shaft

p [-] = number of pole-pairs.

Substituting N_s by its value and considering the first relation and the fact that there is only one pole-pair, the equation for the critical torsional velocities of the system becomes:

$$N = 60\ F - 375 \tag{8}$$

During the asynchronous start-up procedure, it is therefore necessary to keep away from those frequencies by which the above equation can by satisfied, in order to avoid torsional vibrations which might cause a failure of the thin shaft.

Once arrived at synchronous operation, (~ 5000 r.p.m.), mechanical excitation frequency Fe is zero as can easily be seen from the expression for Fe, and therefore there are no more critical velocities of torsion.

2. CALCULATION OF CRITICAL FLEXIONAL VELOCITIES

To simplify the calculation while still adhering very closely to the real conditions, the system in Fig. 1 has been reduced to that shown in Fig. 4.

For the reason given in the introduction, we shall consider the three following cases:

(A) System as in Fig. 4, loaded at its free end with the rotor of weight P = 30 Kg. The gyroscopic effet due to the rotor and the traction effect due to the weight of the rotor F = P = 30 Kg are both ignored.

(B) System as above, taking into consideration the gyroscopic effect due to the rotor but ignoring the traction effect.

(C) System as at (A) taking into consideration both the gyroscopic and the traction effects.

The IBM 7090 computer was used for the solution of each of these three cases, with which we shall now deal.

2.1 Calculation of the critical velocities of the system ignoring both gyroscopic and traction effects

We know that, in the case under consideration, the basic equation for the critical velocities in respect of a shaft, of constant cross-section, fixed only at its ends and subjected to a uniformly-distributed load of weight p

C.C.R.
ISPRA

EURATOM

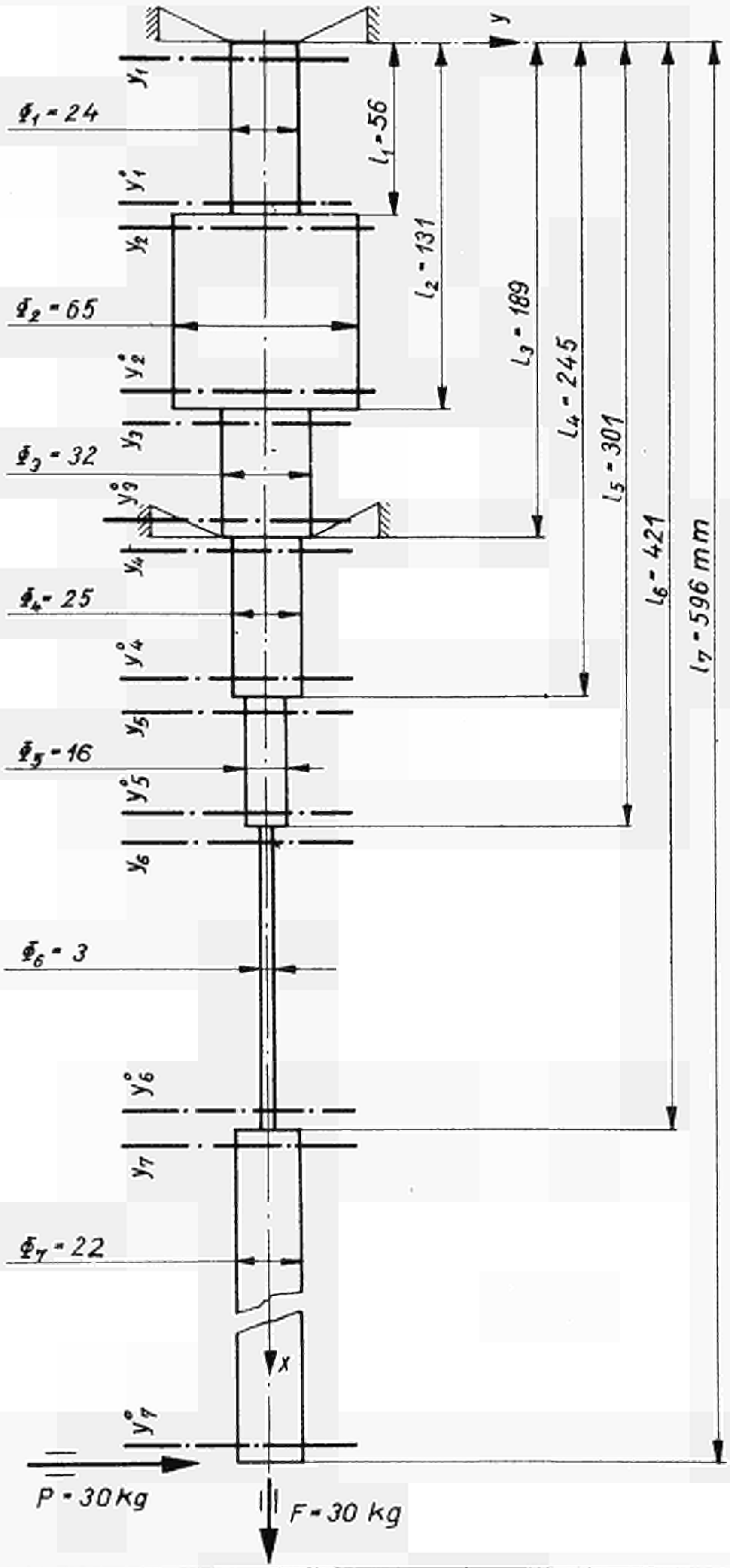

$$S_1 = \frac{\pi \cdot 2{,}4^2}{4} \cong 4{,}5\ cm^2$$
$$S_2 = \frac{\pi \cdot 6{,}5^2}{4} \cong 33\ cm^2$$
$$S_3 = \frac{\pi \cdot 3{,}2^2}{4} \cong 8\ cm^2$$
$$S_4 = \frac{\pi \cdot 2{,}5^2}{4} \cong 4{,}9\ cm^2$$
$$S_5 = \frac{\pi \cdot 1{,}6^2}{4} \cong 2{,}54\ cm^2$$
$$S_6 = \frac{\pi \cdot 0{,}3^2}{4} \cong 0{,}07\ cm^2$$
$$S_7 = \frac{\pi \cdot 2{,}2^2}{4} \cong 3{,}8\ cm^2$$

$$J_1 = \frac{\pi \cdot 2{,}4^4}{64} \cong 1{,}62\ cm^4$$
$$J_2 = \frac{\pi \cdot 6{,}5^4}{64} = 87{,}5\ cm^4$$
$$J_3 = \frac{\pi \cdot 3{,}2^4}{64} = 5{,}14\ cm^4$$
$$J_4 = \frac{\pi \cdot 2{,}5^4}{64} \cong 1{,}92\ cm^4$$
$$J_5 = \frac{\pi \cdot 1{,}6^4}{64} \cong 0{,}32\ cm^4$$
$$J_6 = \frac{\pi \cdot 0{,}3^4}{64} \cong 0{,}0004\ cm^4$$
$$J_7 = \frac{\pi \cdot 2{,}2^4}{64} \cong 1{,}15\ cm^4$$

$$\gamma \cong \frac{0{,}008\ kg}{cm^3}$$
$$g = \frac{981\ cm}{sec^2}$$
$$E \cong \frac{2\,000\,000\ kg}{cm^2}$$

Fig. 4

7.10.63

per unit of length, in the conditions assumed usually by the analysis of stress and strain is (3) - (4) - (5) - (11) - (12):

$$\frac{d^4 y}{dx^4} = m^4 y \qquad (9)$$

with

$$m^4 = \frac{\Omega^2 \, p}{E \, J \, g} \qquad (10)$$

where:

- $p = S\gamma$ = weight of shaft per unit length
- S = cross-section of shaft
- γ = specific gravity of shaft material
- E = modulus of elasticity of shaft material
- J = moment of inertia of cross-section of shaft
- g = acceleration due to gravity
- Ω = angular velocity of shaft.

The integral equation (9) has the value

$$y = A \cosh m\,x + B \sinh m\,x + C \cos m\,x + D \sin m\,x \qquad (11)$$

where A, B, C, D are constants which depend on the boundary conditions.

Taking these into consideration we can always write a sufficient number of equations containing the constants and the m; we then cancel out the constant values and obtain an equation in m whose solutions, substituted in equation (10), enable us to find the critical velocities of the shaft.

In respect of a shaft made up of a number of lengths of various diameter and fixed at several points, equation (11) is valid for each length and for each contiguous length confined by a point of attachment; hence we must write as many separate equations as there are lengths of different diameter and lengths confined by a point of attachment. In the case in question (Fig. 4) denoting with the indices 1, 2, ..., 7, the values relating to the 1st, 2nd ... 7th length, we have the seven following equations:

$$
\begin{aligned}
y &= A_1 \cosh m_1 x + B_1 \sinh m_1 x + C_1 \cos m_1 x + D_1 \sin m_1 x \\
y &= A_2 \cosh m_2 x + B_2 \sinh m_2 x + C_2 \cos m_2 x + D_2 \sin m_2 x \\
&\ldots\ldots\ldots\ldots\ldots\ldots\ldots\ldots\ldots\ldots\ldots\ldots \\
&\ldots\ldots\ldots\ldots\ldots\ldots\ldots\ldots\ldots\ldots\ldots\ldots \\
&\ldots\ldots\ldots\ldots\ldots\ldots\ldots\ldots\ldots\ldots\ldots\ldots \\
&\ldots\ldots\ldots\ldots\ldots\ldots\ldots\ldots\ldots\ldots\ldots\ldots \\
y &= A_7 \cosh m_7 x + B_7 \sinh m_7 x + C_7 \cos m_7 x + D_7 \sin m_7 x
\end{aligned}
\qquad (12)
$$

Bearing in mind that the angular velocity Ω is common to all the lengths and that it is related to the various $m_1, \ldots, m_7$; $S_1, \ldots, S_7$; $J_1, \ldots, J_7$ by equation (10), we can write:

$$
\frac{m_1^4 E J_1 g}{S_1 \gamma} = \frac{m_2^4 E J_2 g}{S_2 \gamma} = \frac{m_3^4 E J_3 g}{S_3 \gamma} = \frac{m_4^4 E J_4 g}{S_4 \gamma} =
$$

$$
= \frac{m_5^4 E J_5 g}{S_5 \gamma} = \frac{m_6^4 E J_6 g}{S_6 \gamma} = \frac{m_7^4 E J_7 g}{S_7 \gamma}
$$

from which we obtain:

$$
\begin{aligned}
m_2 &= m_1 \sqrt[4]{\frac{S_2 J_1}{S_1 J_2}} = \varphi\, m_1 \\
m_3 &= m_1 \sqrt[4]{\frac{S_3 J_1}{S_1 J_3}} = \xi\, m_1 \\
m_4 &= m_1 \sqrt[4]{\frac{S_4 J_1}{S_1 J_4}} = \tau\, m_1
\end{aligned}
\qquad (13)
$$

$$m_5 = m_1 \sqrt[4]{\frac{S_5\ J_1}{S_1\ J_5}} = \psi\ m_1$$

$$m_6 = m_1 \sqrt[4]{\frac{S_6\ J_1}{S_1\ J_6}} = \eta\ m_1 \qquad (13)$$

$$m_7 = m_1 \sqrt[4]{\frac{S_7\ J_1}{S_1\ J_7}} = \alpha\ m_1$$

The numerical values of $S_1,\dots,S_7$; $J_1,\dots,J_7$; g; γ; and E are shown in Fig.4.

The conditions at the limits of each length can be written, bearing in mind the following:

- at a single support, deflection and bending moment are nil; that is, given y as the generic deflection and M the bending moment,

$$\begin{cases} y = 0 \\ M = E\ J\ y'' = 0 \end{cases}$$

- at the point of junction between two sections of different diameter, deflection y, gradient $\frac{dy}{dx}$, bending moment M and shearing stress T are equal for the two sections, so that

$$y_i = y_{i+1}$$

$$y'_i = y'_{i+1}$$

$$M_i = E\ J_i y''_i = E\ J_{i+1}\ y''_{i+1} = M_{i+1}$$

$$T_i = E\ J_i\ y'''_i = E\ J_{i+1}\ y'''_{i+1} = T_{i+1}$$

In our case, if we denote the characteristic values of the beam at the end of each length with the superscript index zero, and the same values at the beginning of each length without the index zero (Fig. 4), we have:

(1) <u>for x = 0</u>

$$\begin{cases} y_1 = 0 \\ y_1'' = 0 \end{cases}$$

(2) <u>for x = l_1</u>

$$\begin{cases} y_1^o = y_2 \\ y_1^{o\,\prime} = y_2' \\ E\ J_1\ y_1^{o\,\prime\prime} = E\ J_2\ y_2'' \\ E\ J_1\ y_1^{o\,\prime\prime\prime} = E\ J_2\ y_2''' \end{cases}$$

(3) <u>for x = l_2</u>

$$\begin{cases} y_2^o = y_3 \\ y_2^{o\,\prime} = y_3' \\ E\ J_2\ y_2^{o\,\prime\prime} = E\ J_3 y_3'' \\ E\ J_2\ y_2^{o\,\prime\prime\prime} = E\ J_3 y_3''' \end{cases}$$

(4) <u>for x = l_3</u>

$$\begin{cases} y_3^o = 0 \\ y_4 = 0 \\ y_3^{o\,\prime} = y_4' \\ E\ J_3\ y_3^{o\,\prime\prime} = E\ J_4\ y_4'' \end{cases}$$

(5) <u>for x = l_4</u>

$$\begin{cases} y_4^o = y_5 \\ y_4^{o\,\prime} = y_5' \\ E\ J_4\ y_4^{o\,\prime\prime} = E\ J_5\ y_5'' \\ E\ J_4\ y_4^{o\,\prime\prime\prime} = E\ J_5\ y_5''' \end{cases}$$

(6) <u>for x = l_5</u>

$$\begin{cases} y_5^o = y_6 \\ y_5^{o\,\prime} = y_6' \\ E\ J_5\ y_5^{o\,\prime\prime} = E\ J_6\ y_6'' \\ E\ J_5\ y_5^{o\,\prime\prime\prime} = E\ J_6\ y_6''' \end{cases}$$

(7) <u>for x = l_6</u>

$$\begin{cases} y_6^o = y_7 \\ y_6^{o\,\prime} = y_7' \\ E\ J_6\ y_6^{o\,\prime\prime} = E\ J_7\ y_7'' \\ E\ J_6\ y_6^{o\,\prime\prime\prime} = E\ J_7\ y_7''' \end{cases}$$

(8) <u>for x = l_7</u>

$$\begin{cases} y_7^{o\,\prime\prime} = 0 \\ y_7^{o\,\prime\prime\prime} = R\ \alpha^4\ m_1^4\ y_7^o \end{cases}$$

The last condition at the limits, for x = l_7, can be found, since we know (ref. 5) that:

$$E\,J_7\,y_7^{o'''} = -\,P/g\,\Omega^2\,y_7^o$$

in which we substitute the value given by equation (9) for Ω^2, i.e.

$$\Omega^2 = \frac{m_7^4\,E\,J_7\,g}{S_7\,\gamma}$$

and, from the last of equations (13), we obtain

$$E\,J_7\,y_7^{o'''} = -\,\frac{P}{g}\,\frac{m_7^4\,E\,J_7\,g}{S_7\,\gamma}\,y_7^o = -\,\frac{P\,\alpha^4\,m_1^4}{S_7\,\gamma}\,y_7^o$$

whence the said and last condition with

$$R = -\,\frac{P}{S_7\gamma} = -\,\frac{30}{3.8 \times 0.008} \simeq -\,986\ \text{cm}$$

Equations (12) and (13), together with the conditions at the limits of each length as written above, enable us to write a homogeneous set of 28 equations in the 28 unknowns $A_1 \ldots\ldots A_7$, $B_1 \ldots\ldots B_7$, $C_1 \ldots\ldots C_7$, $D_1 \ldots\ldots D_7$.

Having constructed the determinant of the coefficients, we note that it is a function of the single parameter m_1; for all the values of this which cancel the determinant, (10) enables us to calculate the critical flexional angular velocities Ω and hence the critical rpm values of our system.

The foregoing is the standard method of calculating the critical flexional velocities. In practice it is difficult to programme for the IBM 7090, so that we found it preferable, from that standpoint, to use the method set out below as it is far more convenient. It consists, very simply, in expressing the final conditions of the beam in question as a function of the initial conditions, taking into account the conditions at the limits as written above. (For detailed explanation of the method right up to the feeding into the IBM 7090, the reader is referred to the report by Messrs. MONTEROSSO and DI COLA, not yet published).

Equation (9), applied to the 1st beam section, gives

$$y = A_1 \cosh m_1 x + B_1 \sinh m_1 x + C_1 \cos m_1 x + D_1 \sin m_1 x \quad (14)$$

Its successive derivatives up to the third, have the values

$$\begin{aligned} y' &= m_1 A_1 \sinh m_1 x + m_1 B_1 \cosh m_1 x - \\ &\quad - m_1 C_1 \sin m_1 x + m_1 D_1 \cos m_1 x \\ y'' &= m_1^2 A_1 \cos h\, m_1 x + m_1^2 B_1 \sinh m_1 x - \\ &\quad - m_1^2 C_1 \cos m_1 x - m_1^2 D_1 \sin m_1 x \\ y''' &= m_1^3 A_1 \sinh m_1 x + m_1^3 B_1 \cosh m_1 x + \\ &\quad + m_1^3 C_1 \sin m_1 x - m_1^3 D_1 \cos m_1 x \end{aligned} \quad (15)$$

The set formed from (14) and (15) for x = 0 gives:

$$\begin{aligned} y_1 &= A_1 + C_1 \\ y_1' &= m_1 B_1 + m_1 D_1 \\ y_1'' &= m_1^2 A_1 - m_1^2 C_1 \\ y_1''' &= m_1^3 B_1 - m_1^3 D_1 \end{aligned} \quad (16)$$

where y_1, y_1', y_1'', y_1''' are the initial conditions of the beam.

Deriving A_1, B_1, C_1, D_1 from this set and substituting them in the set formed from (14) and (15) we obtain, for $x = l_1$:

$$\begin{aligned} y_1^o &= y_1 \frac{1}{2} (\cosh m_1 l_1) + y_1' \frac{1}{2\, m_1} (\sinh m_1 l_1 + \sin m_1 l_1) + \\ &\quad + y_1'' \frac{1}{2\, m_1^2} (\cosh m_1 l_1 - \cos m_1 l_1) + y_1''' \frac{1}{2\, m_1^3} \cdot \\ &\quad (\sinh m_1 x - \sin m_1 x) \end{aligned}$$

$$y_1^{o'} = y_1 \frac{m_1}{2} (\sinh m_1 l_1 - \sin m_1 l_1) + y_1' \frac{1}{2} (\cosh m_1 l_1 + \cos m_1 l_1) + y_1'' \frac{1}{2m_1} (\sinh m_1 l_1 + \sin m_1 l_1) + y_1''' \frac{1}{2 m_1^2} (\cosh m_1 x - \cos m_1 x)$$

$$y_1^{o''} = y_1 \frac{m_1^2}{2} (\cosh m_1 l_1 - \cos m_1 l_1) + y_1' \frac{m_1}{2} (\sinh m_1 l_1 - \sin m_1 l_1) + y_1'' \frac{1}{2} (\cosh m_1 l_1 + \cos m_1 l_1) + y_1''' \frac{1}{2 m_1} (\sinh m_1 l_1 + \sin m_1 l_1)$$

$$y_1^{o'''} = y_1 \frac{m_1^3}{2} (\sinh m_1 l_1 + \sin m_1 l_1) + y_1' \frac{m_1^2}{2} (\cosh m_1 l_1 - \cos m_1 l_1) + y_1'' \frac{m_1}{2} (\sinh m_1 l_1 - \sin m_1 l_1) + y_1''' \frac{1}{2} (\cosh m_1 l_1 + \cos m_1 l_1)$$

Bearing in mind the above-mentioned conditions at the limits for the point $x = 0$, we get:

$$
\begin{array}{c}
y_1^{o} \\
y_1^{o'} \\
y_1^{o''} \\
y_1^{o'''}
\end{array}
=
\left|
\begin{array}{cccc}
\frac{1}{2}(\cosh m_1 l_1 + \cos m_1 l_1) & \frac{1}{2m_1}(\sinh m_1 l_1 + \sin m_1 l_1) & \frac{1}{2m_1^2}(\cosh m_1 l_1 - \cos m_2 l_1) & \frac{1}{2m_1^3}(\sinh m_1 l_1 - \sin m_1 l_1) \\
\frac{m_1}{2}(\sinh m_1 l_1 - \sin m_1 l_1) & \frac{1}{2}(\cosh m_1 l_1 + \cos m_1 l_1) & \frac{1}{2m_1}(\sinh m_1 l_1 + \sin m_1 l_1) & \frac{1}{2m_1^2}(\cosh m_2 l_1 - \cos m_1 l_1) \\
\frac{m_1^2}{2}(\cosh m_1 l_1 - \cos m_1 l_1) & \frac{m_1}{2}(\sinh m_1 l_1 - \sin m_1 l_1) & \frac{1}{2}(\cosh m_1 l_1 + \cos m_1 l_1) & \frac{1}{2m_1}\sinh m_1 l_1 + \sin m_1 l_1) \\
\frac{m_1^3}{2}(\sinh m_1 l_1 + \sin m_1 l_1) & \frac{m_1^2}{2}(\cosh m_1 l_1 - \cos m_1 l_1) & \frac{m_1}{2}(\sin m_1 l_1 - \sin m_1 l_1) & \frac{1}{2}(\cosh m_1 l_1 + \cos m_1 l_1)
\end{array}
\right|
\begin{array}{c}
0 \\
y_1' \\
0 \\
y_1'''
\end{array}
\qquad (17)
$$

which represent the value and respective derivatives of y at the end of the first beam-length as a function of the initial conditions.

For the second beam-length, we get:

$$y = A_2 \cosh m_2 x + B_2 \sinh m_2 x + C_2 \cos m_2 x + D_2 \sin m_2 x$$

$$y' = m_2 A_2 \sinh m_2 x + m_2 B_2 \cosh m_2 x - m_2 C_2 \sin m_2 x + $$
$$+ m_2 D_2 \cos m_2 x$$

$$y'' = m_2^2 A_2 \cosh m_2 x + m_2^2 B_2 \sinh m_2 x - \qquad (18)$$
$$- m_2^2 C_2 \cos m_2 x - m_2^2 D_2 \sin m_2 x$$

$$y''' = m_2^3 A_2 \sinh m_2 x + m_2^3 B_2 \cosh m_2 x +$$
$$+ m_2^3 C_2 \sin m_2 x - m_2^3 D_2 \cos m_2 x$$

When $x = l_1$, we obtain

$$y_2 = A_2 \cosh m_2 l_1 + B_2 \sinh m_2 l_1 + C_2 \cos m_2 l_1 + D_2 \sin m_2 l_1$$

$$y_2' = m_2 A_2 \sinh m_2 l_1 + m_2 B_2 \cosh m_2 l_1 - m_2 C_2 \sin m_2 l_2 +$$
$$+ m_2 D_2 \cos m_2 l_1$$

$$y_2'' = m_2^2 A_2 \cosh m_2 l_1 + m_2^2 B_2 \sinh m_2 l_1 -$$
$$- m_2^2 C_2 \cos m_2 l_1 - m_2^2 D_2 \sin m_2 l_1$$

$$y_2''' = m_2^3 A_2 \sinh m_2 l_1 + m_2^3 B_2 \cosh m_2 l_1 +$$
$$+ m_2^3 C_2 \sin m_2 l_1 - m_2^3 D_2 \cos m_2 l_1$$

Deriving A_2, B_2, C_2, D_2 from this set and substituting them in equations (18), we obtain for $x = l_2$, after certain transformations:

$$
\begin{cases}
y_2^{o} = y_2 \frac{1}{2}\left[\cosh m_2(l_2-l_1) + \cos m_2(l_2-l_1)\right] + y_2^{I}\frac{1}{2m_2}\left[\sinh m_2(l_2-l_1) + \sin m_2(l_2-l_1)\right] \; y_2^{II}\frac{1}{2m_2^2}\left[\cosh m_2(l_2-l_1) - \cos m_2(l_2-l_1)\right] + y_2^{III}\frac{1}{2m_2^3}\left[\sinh m_2(l_2-l_1) - \sin m_2(l_2-l_1)\right] \\[2ex]
y_2^{o'} = y_2 \frac{m_2}{2}\left[\sinh m_2(l_2-l_1) - \sin m_2(l_2-l_1)\right] + y_2^{I}\frac{1}{2}\left[\cosh m_2(l_2-l_1) + \cos m_2(l_2-l_1)\right] + y_2^{II}\frac{1}{2m_2}\left[\sinh m_2(l_2-l_1) + \sin m_2(l_2-l_1)\right] + y_2^{III}\frac{1}{2m_2^2}\left[\cosh m_2(l_2-l_1) - \cos m_2(l_2-l_1)\right] \\[2ex]
y_2^{o''} = y_2 \frac{m_2^2}{2}\left[\cosh m_2(l_2-l_1) - \cos m_2(l_2-l_1)\right] + y_2^{I}\frac{m_2}{2}\left[\sinh m_2(l_2-l_1) - \sin m_2(l_2-l_1)\right] + y_2^{II}\frac{1}{2}\left[\cosh m_2(l_2-l_1) + \cos m_2(l_2-l_1)\right] + y_2^{III}\frac{1}{2m_2}\left[\sinh m_2(l_2-l_1) + \sin m_2(l_2-l_1)\right] \\[2ex]
y_2^{o'''} = y_2 \frac{m_2^3}{2}\left[\sinh m_2(l_2-l_1) + \sin m_2(l_2-l_1)\right] + y_2^{I}\frac{m_2^2}{2}\left[\cosh m_2(l_2-l_1) - \cos m_2(l_2-l_1)\right] + y_2^{II}\frac{m_2}{2}\left[\sinh m_2(l_2-l_1) - \sin m_2(l_2-l_1)\right] + y_2^{III}\frac{1}{2}\left[\cosh m_2(l_2-l_1) + \cos m_2(l_2-l_1)\right]
\end{cases}
$$

Which can be written :

$$
\begin{vmatrix} y_2^{o} \\ y_2^{o'} \\ y_2^{o''} \\ y_2^{o'''} \end{vmatrix}
\begin{matrix}
\frac{1}{2}\left[\cosh m_2(l_2-l_1)+\cos m_2(l_2-l_1)\right] & \frac{1}{2m_2}\left[\sinh m_2(l_2-l_1)+\sin m_2(l_2-l_1)\right] & \frac{1}{2m_2^2}\left[\cosh m_2(l_2-l_1)-\cos m_2(l_2-l_1)\right] & \frac{1}{2m_2^3}\left[\sinh m_2(l_2-l_1)-\sin m_2(l_2-l_1)\right] \\
\frac{m_2}{2}\left[\sinh m_2(l_2-l_1)-\sin m_2(l_2-l_1)\right] & \frac{1}{2}\left[\cosh m_2(l_2-l_1)+\cos m_2(l_2-l_1)\right] & \frac{1}{2m_2}\left[\sinh m_2(l_2-l_1)+\sin m_2(l_2-l_1)\right] & \frac{1}{2m_2^2}\left[\cosh m_2(l_2-l_1)-\cos m_2(l_2-l_1)\right] \\
\frac{m_2^2}{2}\left[\cosh m_2(l_2-l_1)-\cos m_2(l_2-l_1)\right] & \frac{m_2}{2}\left[\sinh m_2(l_2-l_1)-\sin m_2(l_2-l_1)\right] & \frac{1}{2}\left[\cosh m_2(l_2-l_1)+\cos m_2(l_2-l_1)\right] & \frac{1}{2m_2}\left[\sinh m_2(l_2-l_1)+\sin m_2(l_2-l_1)\right] \\
\frac{m_2^3}{2}\left[\sinh m_2(l_2-l_1)+\sin m_2(l_2-l_1)\right] & \frac{m_2^2}{2}\left[\cosh m_2(l_2-l_1)-\cos m_2(l_2-l_1)\right] & \frac{m_2}{2}\left[\sinh m_2(l_2-l_1)-\sin m_2(l_2-l_1)\right] & \frac{1}{2}\left[\cosh m_2(l_2-l_1)+\cos m_2(l_2-l_1)\right]
\end{matrix}
\begin{vmatrix} y_2 \\ y_2' \\ y_2'' \\ y_2''' \end{vmatrix} \tag{19}
$$

The conditions at the limits of the length l_1 give:

$$y_1^{o} = y_2$$

$$y_1^{o'} = y_2$$

$$\frac{J_1}{J_2} y_1^{o''} = y_2''$$

$$\frac{J_1}{J_2} y_1^{o'''} = y_2$$

Which is the same as:

$$
\begin{matrix} y_2 \\ y_2' \\ y_2'' \\ y_2''' \end{matrix}
=
\begin{vmatrix}
1 & 0 & 0 & 0 \\
0 & 1 & 0 & 0 \\
0 & 0 & \frac{J_1}{J_2} & 0 \\
0 & 0 & 0 & \frac{J_1}{J_2}
\end{vmatrix}
\cdot
\begin{matrix} y_1^{o} \\ y_1^{o'} \\ y_1^{o''} \\ y_1^{o'''} \end{matrix}
\tag{20}
$$

By substituting expression (20) for y_2, y_2', y_2'', y_2''' in expression (19), and bearing in mind the expression (17) for y_1^0, $y_1^{0'}$, $y_1^{0''}$, $y_1^{0'''}$, we obtain the value and respective derivatives of y up to the end of the second beam-length as a function of the initial conditions:

$$
\begin{vmatrix} y_2^0 \\ y_2^{0'} \\ y_2^{0''} \\ y_2^{0'''} \end{vmatrix}
=
\begin{vmatrix}
\frac{1}{2}\left[\cosh m_2(l_2-l_1)+\cos m_2(l_2-l_1)\right] & \frac{1}{2m_2}\left[\sinh m_2(l_2-l_1)+\sin m_2(l_2-l_1)\right] & \frac{1}{2m_2^2}\left[\cosh m_2(l_2-l_1)-\cos m_2(l_2-l_1)\right] & \frac{1}{2m_2^3}\left[\sinh m_2(l_2-l_1)-\sin m_2(l_2-l_1)\right] \\
\frac{m_2}{2}\left[\sinh m_2(l_2-l_1)-\sin m_2(l_2-l_1)\right] & \frac{1}{2}\left[\cosh m_2(l_2-l_1)+\cos m_2(l_2-l_1)\right] & \frac{1}{2m_2}\left[\sinh m_2(l_2-l_1)+\sin m_2(l_2-l_1)\right] & \frac{1}{2m_2^2}\left[\cosh m_2(l_2-l_1)-\cos m_2(l_2-l_1)\right] \\
\frac{m_2^2}{2}\left[\cosh m_2(l_2-l_1)-\cos m_2(l_2-l_1)\right] & \frac{m_2}{2}\left[\sinh m_2(l_2-l_1)-\sin m_2(l_2-l_1)\right] & \frac{1}{2}\left[\cosh m_2(l_2-l_1)+\cos m_2(l_2-l_1)\right] & \frac{1}{2m}\left[\sinh m_2(l_2-l_1)+\sin m_2(l_2-l_1)\right] \\
\frac{m_2^3}{2}\left[\sinh m_2(l_2-l_1)+\sin m_2(l_2-l_1)\right] & \frac{m_2^2}{2}\left[\cosh m_2(l_2-l_1)-\cos m_2(l_2-l_1)\right] & \frac{m_2}{2}\left[\sinh m_2(l_2-l_1)-\sin m_2(l_2-l_1)\right] & \frac{1}{2}\left[\cosh m_2(l_2-l_1)+\sin m_2(l_2-l_1)\right]
\end{vmatrix}
\cdot
$$

$$
\begin{vmatrix}
1 & 0 & 0 & 0 \\
0 & 1 & 0 & 0 \\
0 & 0 & \frac{J}{J} & 0 \\
0 & 0 & 0 & \frac{J}{J}
\end{vmatrix}
\cdot
\begin{vmatrix}
\frac{1}{2}(\cosh m_1 l_1+\cos m_1 l_1) & \frac{1}{2m_1}(\sinh m_1 l_1+\sin m_1 l_1) & \frac{1}{2m_1^2}(\cosh m_1 l_1-\cos m_2 l_1) & \frac{1}{2m_1^3}(\sinh m_1 l_1-\sin m_1 l_1) \\
\frac{m_1}{2}(\sinh m_1 l_1-\sin m_1 l_1) & \frac{1}{2}(\cosh m_1 l_1+\cos m_1 l_1) & \frac{1}{2m_1}(\sinh m_1 l_1+\sin m_1 l_1) & \frac{1}{2m_1^2}(\cosh m_2 l_1-\cos m_1 l_1) \\
\frac{m_1^2}{2}(\cosh m_1 l_1-\cos m_1 l_1) & \frac{m_1}{2}(\sinh m_1 l_1-\sin m_1 l_1) & \frac{1}{2}(\cosh m_1 l_1+\cos m_1 l_1) & \frac{1}{2m_1}(\sinh m_1 l_1+\sin m_1 l_1) \\
\frac{m_1^3}{2}(\sinh m_1 l_1+\sin m_1 l_1) & \frac{m_1^2}{2}(\cosh m_1 l_1-\cos m_1 l_1) & \frac{m_1}{2}(\sinh m_1 l_1-\sin m_1 l_1) & \frac{1}{2}(\cosh m_1 l_1+\cos m_1 l_1)
\end{vmatrix}
\begin{vmatrix} 0 \\ y_1' \\ 0 \\ y_1''' \end{vmatrix}
$$

Proceeding in the same way for the remaining beam-lengths, we obtain the value and respective derivatives at the end of the last length in terms of the initial conditions; i.e. we obtain:

$$\begin{vmatrix} y_7^{o} \\ y_7^{o'} \\ y_7^{o''} \\ y_7^{o'''} \end{vmatrix} = \begin{vmatrix} A \end{vmatrix} \cdot \begin{vmatrix} B \end{vmatrix} \cdot \begin{vmatrix} C \end{vmatrix} \cdots\cdots \begin{vmatrix} N \end{vmatrix} \begin{matrix} 0 \\ y_1' \\ 0 \\ y_7''' \end{matrix} \qquad (21)$$

where A, B, C, ... , N are matrices calculated as above. With the conditions at the limits for $x = l_7$ and the relations (13) which correlate the various m_2, m_3, ... , m_7 with m_1, equation (21) when solved by the IBM 7090 for the speed range 0 - 40,000 rpm, gave two values of m_1, to which the two following critical velocities correspond:

1st critical velocity: $ncr_1 \simeq 18$ rpm

2nd critical velocity: $ncr_2 \simeq 2{,}200$ rpm.

2.2 <u>Calculation of the critical velocities of the system, taking into account the gyroscopic effect but disregarding the traction effect</u>

In the treatment of this second case the gyroscopic effect of the flywheel located at the free end of the beam, which was disregarded in the first case, is taken into consideration.

This effect does not alter the differential equation (9), which therefore remains the same in this case, but only the limit conditions at the extreme point $x = l_7$ at which the flywheel is applied; we shall now determine these conditions.

In cases where concentrated loads such as pulleys or flywheels are applied to a shaft, when writing the equations at the limits for two contiguous lengths limited by a load, we must bear in mind not only that the ordinates and the gradients of the elastic curve and the shearing stresses, as calculated from the two equations relating to the two lengths, must work out equal, but also that there exists between the moments calculated below and above the loaded section the relation

$$M_v - M_m = \Omega^2 \, P/g \; \rho^2 \; y'^{(5)} \qquad (22)$$

where P, g, Ω^2 have the same meaning as before and ρ is the radius of gyration of the flywheel or pulley.

In our case, since the flywheel is at the free end of the beam, (22) is reduced to

$$- M_m = \Omega^2 \, P/g \; \rho^2 \; y_7^{o\,\prime}$$

and, replacing M_m by its value,

$$E \, J_7 \, y_7^{o\,\prime\prime} = - \Omega^2 \, P/g \; \rho^2 \; y_7^{o\,\prime} = - \frac{m_7^4 \, E \, J_7 \, g}{S_7 \, \gamma} \frac{P}{g} \rho^2 \; y_7^{o\,\prime}$$

i.e.

$$y_7^{o\,\prime\prime} = - \frac{\alpha^4 \, m_1^4 \, P \, \rho^2}{S_7 \, \gamma} \; y_7^{o\,\prime} = H \, \alpha^4 \, m^4 \, y_7^{o\,\prime} \qquad (23)$$

where:

$$\rho^2 = \frac{g \, Y_1}{2P} \simeq \frac{981 \times 2.81}{2 \times 30} \simeq 46 \text{ cm}^2$$

$$H \simeq - \frac{P \, \rho^2}{S_7 \, \gamma} \simeq \frac{30 \times 46}{4.16 \times 0.008} \simeq 45{,}500 \text{ cm}^3$$

The limit conditions for

$$x = l_7$$

are therefore in this second case

$$\begin{cases} y_7^{o''} = H\,\alpha^4\,m_1^4\,y_7^{o'} \\ y_7^{o'''} = R\,\alpha^4\,m_1^4\,y_7^{o} \end{cases} \qquad (24)$$

When the calculation was made on the IBM 7090 as described **in section 2.1,** equations (24) being now substituted for the limit conditions at the point $x = l_7$, the following were found for the velocity range 0 - 40,000 rpm:

first critical velocity: ncr_1 = 20 rpm
second critical velocity: ncr_2 = 29,500 rpm

This result shows that the gyroscopic effect has very little influence on the first critical flexional velocity but causes a large increase in the second critical velocity, raising it from the 2,200 rpm of **section** 2.1 **to 29,500 rpm.**

2.3 <u>Calculation of the critical velocities of the system, taking both the gyroscopic and the traction effects into account</u>

In this case account is taken of the gyroscopic effect due to the flywheel of weight P = 30 kg located at the end of the shaft and the effect due to the pull of the **force** F = 30 kg (weight of rotor). The differential equation for each beam-length now has the form:

$$E\,J\,\frac{d^4\,y}{d\,x^4} - F\,\frac{d^2\,y}{d\,x^2} = \frac{S\,\gamma}{g}\,\Omega^2\,y \qquad (4) - (5) \qquad (25)$$

whose integral is

$$y = a\,e^{m^I x} + b\,e^{m^{II} x} + c\,e^{m^{III} x} + d\,e^{m^{IV} x}$$

where m^I .... m^{IV} are the roots of the equation:

$$E\,J\,m^4 - F\,m^2 - \frac{S\,\gamma\,\Omega^2}{g} = 0$$

i.e.

$$m_{(I,\ II,\ III,\ IV)} = \pm \sqrt{\frac{F}{2\,E\,J} \pm \sqrt{\frac{F^2}{4\,E^2\,J^2} + \frac{S\,\gamma\,\Omega^2}{g\,E\,J}}} \qquad (26)$$

From this relation it can be seen that there are two equal real roots of opposite sign, which we call respectively m and -m, and two equal and opposite imaginary roots, which we call ir and -ir.

The integral of equation (25) then becomes

$$y = a\,e^{mx} + b\,e^{-mx} + c\,e^{ir} + d e^{-ir}$$

from which, making the appropriate changes, we obtain the equation:

$$y = A \cosh mx + B \sinh mx + C \cos r\,x + D \sin rx$$

which is valid for each of the seven sections that make up the system under study.

The conditions at the limits of each section are the same as **in section 2.1**, with the exception of those relating to the point $x = l_7$, which has now become:

$$\left.\begin{aligned} E\,J_7\,y_7^{o\,''} &= -\,\Omega^2\,P/g\,\rho^2\,y_7^{o\,'} \\ E\,J_7\,y_7^{o\,'''} &= -\,P/g\,\Omega^2\,y_7^{o} + F\,y_7^{o\,'} \end{aligned}\right\} \qquad (27)$$

The term $F\,y_7^{o\,'}$ represents the component of the pull in the direction of the **y** axis at the point $x = l_7$. It is opposite to the centrifugal force $\frac{P}{g}\,\Omega^2\,y_7^{o}$ due to the flywheel of weight P.

Applying the method of calculation shown in **section 2.1, we** find, as far as the second beam-section:

$$
\begin{bmatrix} y^{\circ} \\ y_2^{\circ\prime} \\ y_2^{\circ\prime\prime} \\ y_2^{\circ\prime\prime\prime} \end{bmatrix}
=
\begin{bmatrix}
\frac{1}{(r_2^2+m_2^2)}\left[r_2^2\cosh m_2(l_2-l_1)+m_2^2\cos r_2(l_2-l_1)\right] & \frac{1}{(r_2^2+m_2^2)}\left[\frac{r_2^2}{m_2}\sinh m_2(l_2-l_1)+\frac{m_2^2}{r_2}\sin r_2(l_2-l_1)\right] & \frac{1}{(r_2^2+m_2^2)}\left[\cosh m_2(l_2-l_1)-\cos r_2(l_2-l_1)\right] & \frac{1}{(r_2^2+m_2^2)}\left[\frac{1}{m_2}\sinh m_2(l_2-l_1)-\frac{1}{r_2}\sin r_2(l_2-l_1)\right] \\
\frac{m_2 r_2}{(r_2^2+m_2^2)}\left[r_2\sinh m_2(l_2-l_1)-m_2\sin r_2(l_2-l_1)\right] & \frac{1}{(r_2^2+m_2^2)}\left[r_2^2\cosh m_2(l_2-l_1)+m_2^2\cos r_2(l_2-l_1)\right] & \frac{1}{(r_2^2+m_2^2)}\left[m_2\sinh m_2(l_2-l_1)+r_2\sin r_2(l_2-l_1)\right] & \frac{1}{(r_2^2+m_2^2)}\left[\cosh m_2(l_2-l_1)-\cos r_2(l_2-l_1)\right] \\
\frac{m_2^2 r_2^2}{(r_2^2+m_2^2)}\left[\cosh m_2(l_2-l_1)-\cos r_2(l_2-l_1)\right] & \frac{m_2 r_2}{(r_2^2+m_2^2)}\left[r_2\sinh m_2(l_2-l_1)-m_2\sin r_2(l_2-l_1)\right] & \frac{1}{(r_2^2+m_2^2)}\left[m_2^2\cosh m_2(l_2-l_1)+r_2^2\cos r_2(l_2-l_1)\right] & \frac{1}{(r_2^2+m_2^2)}\left[m_2\sinh m_2(l_2-l_1)+r_2\sin r_2(l_2-l_1)\right] \\
\frac{m_2^2 r_2^2}{(r_2^2+m_2^2)}\left[m_2\sinh m_2(l_2-l_1)+r_2\sin r_2(l_2-l_1)\right] & \frac{m_2^2 r_2^2}{(r_2^2+m_2^2)}\left[\cosh m_2(l_2-l_1)-\cos r_2(l_2-l_1)\right] & \frac{1}{(r_2^2+m_2^2)}\left[m_2^3\sinh m_2(l_2-l_1)-r_2^3\sin r_2(l_2-l_1)\right] & \frac{1}{(r_2^2+m_2^2)}\left[m_2^2\cosh m_2(l_2-l_1)+r_2^2\cos r_2(l_2-l_1)\right]
\end{bmatrix}
\cdot
\begin{bmatrix} 1 & 0 & 0 & 0 \\ 0 & 1 & 0 & 0 \\ 0 & 0 & \frac{J_1}{J_2} & 0 \\ 0 & 0 & 0 & \frac{J_1}{J_2} \end{bmatrix}
$$

$$
\cdot
\begin{bmatrix}
\frac{1}{r_1^2+m_1^2}(r_1^2\cosh m_1 l_1+m_1^2\cos r_1 l_1) & \frac{1}{r_1^2+m_1^2}\left(\frac{r_1^2}{m_1}\sinh m_1 l_1+\frac{m_1^2}{r_1}\sin r_1 l_1\right) & \frac{1}{r_1^2+m_1^2}(\cosh m_1 l_1-\cos r_1 l_1) & \frac{1}{r_1^2+m_1^2}\left(\frac{1}{m_1}\sinh m_1 l_1-\frac{1}{r_1}\sin r_1 l_1\right) \\
\frac{m_1 r_1}{r_1^2+m_1^2}(r_1\sinh m_1 l_1-m_1\sin r_1 l_1) & \frac{1}{r_1^2+m_1^2}(r_1^2\cosh m_1 l_1+m_1^2\cos r_1 l_1) & \frac{1}{r_1^2+m_1^2}(m_1\sinh m_1 l_1+r_1\sin r_1 l_1) & \frac{1}{r_1^2+m_1^2}(\cosh m_1 l_1-\cos r_1 l_1) \\
\frac{m_1^2 r_1^2}{r_1^2+m_1^2}(\cosh m_1 l_1-\cos r_1 l_1) & \frac{m_1 r_1}{r_1^2+m_1^2}(r_1\sinh m_1 l_1-m_1\sin r_1 l_1) & \frac{1}{r_1^2+m_1^2}(m_1^2\cosh m_1 l_1+r_1^2\cos r_1 l_1) & \frac{1}{r_1^2+m_1^2}(m_1\sinh m_1 l_1+r_1\sin r_1 l_1) \\
\frac{m_1^2 r_1^2}{r_1^2+m_1^2}(m_1\sinh m_1 l_1+r_1\sin r_1 l_1) & \frac{m_1^2 r_1^2}{r_1^2+m_1^2}(\cosh m_1 l_1-\cos r_1 l_1) & \frac{1}{r_1^2+m_1^2}(m_1^3\sin m_1 l_1-r_1^3\sin r_1 l_1) & \frac{1}{r_1^2+m_1^2}(m_1^2\cosh m_1 l_1+r_1^2\cos r_1 l_1)
\end{bmatrix}
\cdot
\begin{bmatrix} 0 \\ y_1' \\ 0 \\ y_1''' \end{bmatrix}
$$

Proceeding in the same way with the remaining lengths we arrive at an expression similar to (21) which gives us the value and respective derivatives of y at the end of the last length as a function of the initial conditions.

Associating with it the limit conditions (27) and the expressions for m_1 ..... m_7 and r_1 ...... r_7 given by (26), the IBM 7090 supplied the two velocities below, for the velocity range 0-40,000 rpm:

first critical velocity: $n\ cr_1 \simeq 64$ rpm
second critical velocity: $n\ cr_2 \simeq 29{,}500$ rpm

This result shows that the traction F changes only the first critical velocity and does not affect the second critical velocity of the system, or rather, its influence on the second critical velocity is very small as compared with that of the gyroscopic effect. Actually, when a calculation was made of the system taking traction effect but not the gyroscopic effect into account, we obtained:

first critical velocity: $n\ cr_1 \simeq 62$ rpm
second critical velocity: $n\ cr_2 \simeq 2{,}800$ rpm

3. CALCULATION OF THE CRITICAL PRECESSION VELOCITIES

The portion of shaft above the small-diameter (3mm) section (see Fig. 1) is extremely rigid with respect to the latter; this is confirmed by calculation and by tests conducted on the rotating system up to failure of the narrow-section.

Hence, for the purpose of calculating the critical precession velocities, no appreciable error will be made by adopting the simplified system shown in Fig. 5.

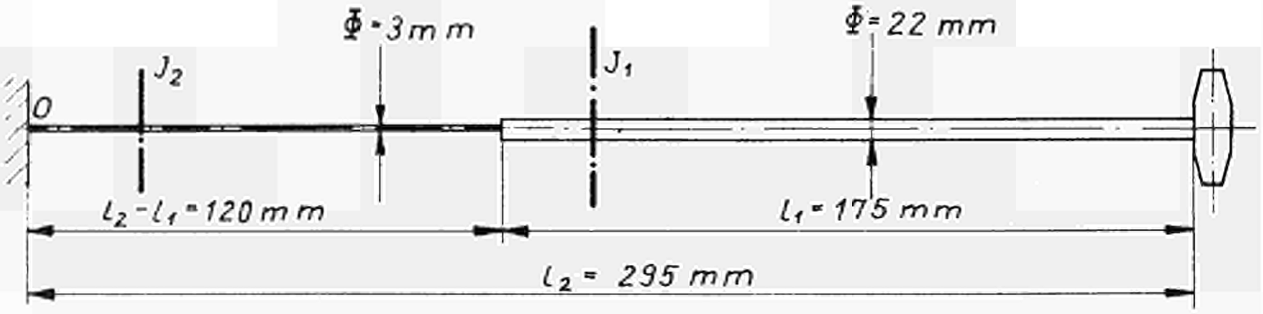

FIG. 5

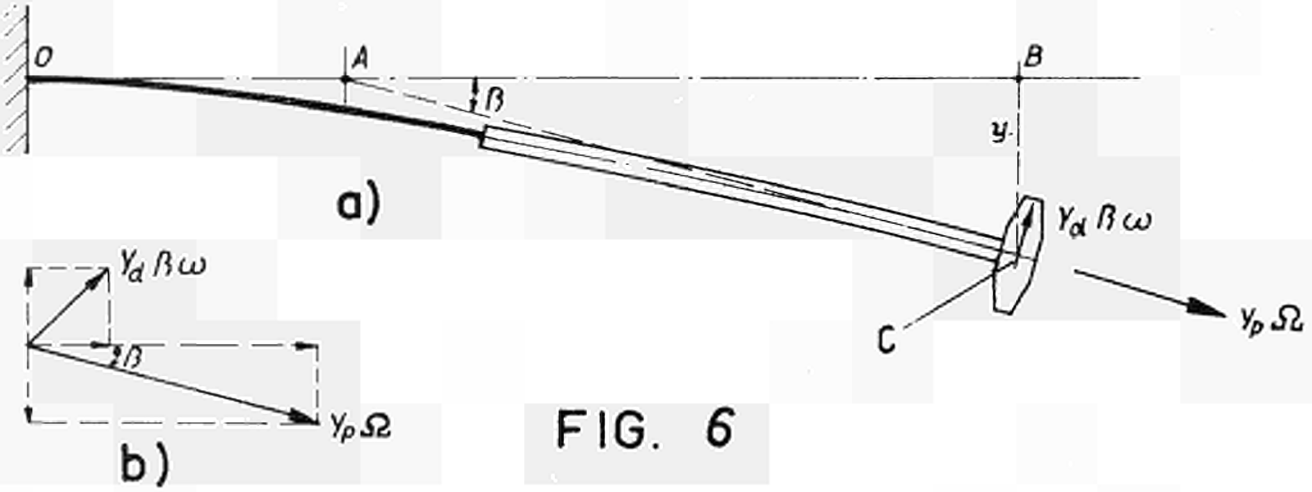

FIG. 6

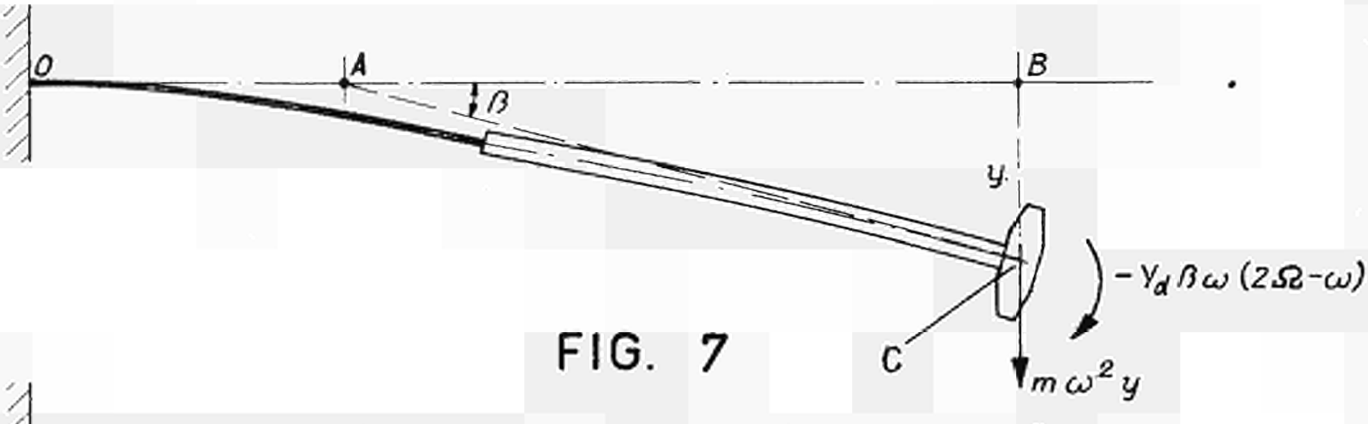

FIG. 7

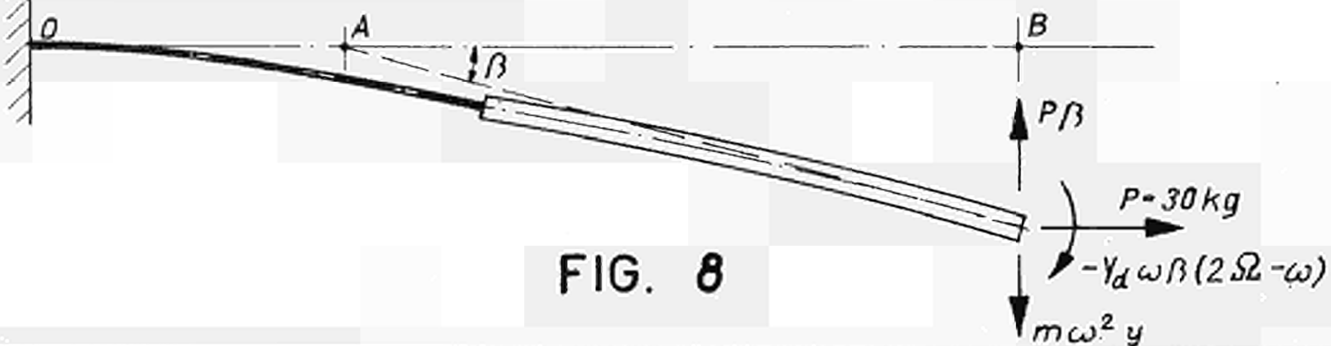

FIG. 8

For the sake of clarity we have thought it advisable here to set out this calculation in three parts, as follows:

(A) calculation of the moment of the forces transmitted from the rotor to the shaft;

(B) equation and calculation of the precession velocities;

(C) determination of the critical precession velocities.

These are dealt with below.

3.1 Calculation of the moment of the forces transmitted from the rotor to the shaft

For the calculation of the critical velocities of bending it was assumed that the rotational speed of the system around the distorted axis is the same as the speed around the straight-lined original axis.

Let us assume now the shaft-rotor system in Fig. 5 has the following velocities:

- precession velocity ω, at which the axis of the shaft, distorted as shown in Fig. 6a, rotates anti-clockwise round the axis OB which corresponds to its non-distorted position;
- rotational velocity Ω around the distorted axis OC, in the same direction as the precession.

Owing to these velocities, the rotor is subjected to two different moments of momentum, which will be calculated separately.

Let us suppose that $\omega = 0$ and $\Omega \neq 0$.

The rotor will then turn without precession around the deformed axis OC so that, given Y_p as its polar moment of inertia with respect to axis OC its angular momentum is the vector $Y_p\ \Omega$ perpendicular to the plane of the rotor and having the direction shown in Fig. 6a.

If $\Omega = 0$ and $\omega \neq 0$ the rotor is subjected to two rotations: one together with the shaft, with angular velocity ω, around the axis OB, its centre of gravity C describing a circle with centre B and radius y, and the other, with angular velocity μ, around one of its diameters which is perpendicular at C to AC which is perpendicular to the mean plane of the rotor, the shaft always remaining perpendicular at C to the rotor during precession.

The first rotation sets up the centrifugal force $m\ \omega^2\ y$ (Fig. 7), m being the rotor mass; while the second causes the angular momentum due to precession.

The latter moment is the product of $\mu\ Y_d$, where Y_d is the moment of inertia of the rotor respect to its diameter. Let us calculate the values of μ and Y_d. In the case of a thin disc

$$Y_d = Y_p/2$$

a relation which is sufficiently applicable to the rotor under consideration. The angular velocity μ of the rotor is not so easy to calculate.

Bearing in mind, however, that during precession the shaft always remains perpendicular at C to the rotor, we see that the straight line AC (perpendicular to the rotor), forming the angle β with the axis OB, rotates at the same angular velocity μ as the rotor. Thus if we determine the angular velocity of AC we shall have found that of the rotor. As it moves, the straight line AC describes a cone, with vertex A, and its end C has a velocity of ω y.

At time t = 0, shown in Fig. 6a, the straight line AC is in the plane of the diagram and the velocity of its point C is perpendicular to the latter. After a time dt, point C is lower than the plane of the diagram by the quantity ω y d t. The angle between the two positions of the straight line AC is then ω y d t/AC and since y/AC = β, if β is small, the angle through which AC rotates in the time dt is ω β d t, and the angular velocity of the straight line AC (and so of the rotor) is

$$\mu = \omega \beta$$

The angular momentum due to precession is then the vector $Y_d \omega \beta$, having the direction and sense indicated in Fig. 6a.

Let us break down each of the angular momentum vectors $Y_p \Omega$ and $Y_d \omega \beta$ into the two components (Fig. 6b) parallel and perpendicular to the axis OB. The total angular momentum to which the rotor is subjected is given by the two vectors

$$Y_p \Omega \cos \beta + Y_d \omega \beta \sin \beta \text{ parallel to axis OB}$$

$$Y_p \Omega \sin \beta - Y_d \omega \beta \cos \beta \text{ perpendicular to axis OB}$$

Where β is assumed to be small, these become respectively:

$$Y_p \Omega + Y_d \omega \beta^2 \qquad \text{parallel to axis OB}$$

$$Y_p \Omega \beta - Y_d \omega \beta = Y_d \beta(2 \Omega - \omega) \text{ perpendicular to axis OB}$$

The first (parallel to axis OB) rotates parallel to itself around the axis OB, describing a circle of radius Y, and its length remains invariable throughout its movement, so that its derivative with respect to time is zero.

The second (perpendicular to the axis OB), on the other hand, describes a circle with centre B as it rotates. At time $t = 0$, this vector is in the plane of the diagram; after a time dt it forms a downward angle of ω dt with this plane.

It thus undergoes a variation given by the product of this vector and ω dt, which is

$$Y_d \ \beta(2\Omega-\omega)\omega \ dt$$

The derivative of this vector with respect to time is

$$Y_d \ \beta(2\Omega-\omega)\omega$$

So this expression represents the derivative with respect to time of the total angular momentum to which the rotor is subjected.

According to the familiar theorem of angular momentum of rational mechanics (Ref. 6), the above expression is equal to the moment of the forces transmitted from the shaft to the rotor and so, by the law of action and reaction, equal and opposite to the moment of the forces transmitted from the rotor to the shaft, i.e. the couple the direction of which is shown in Fig. 7.

3.2 Equation and calculation of the precession velocities

On the assumption always made, likening the rotor to a thin disc, the following forces are applied to the end of the shaft to which it is attached:

- the moment $- Y_d \ \beta\omega(2\Omega-\omega)$
- the centrifugal force $m \ \omega^2 \ y$
- the traction force $F = P = 30$ kg due to the weight P of the rotor when the system is in the vertical position.

The last-named force gives the component $P\ \beta$ (Fig. 8) which is perpendicular to the axis OB, and is constantly opposite to the centrifugal force $m\ \omega^2\ y$.

Denoting by:

α_{11} the deflection of the shaft at the free end where the disc is attached, due to the application of a unit load at that point;

α_{12} the deflection of the shaft at the free end, due to the application of a unit moment at that point; or the angle formed by the shaft with the axis OB at the free end, due to the application of a unit moment at that point;

α_{22} the angle formed by the shaft with the axis OB at the free end, due to the application of a unit moment at that point;

and ignoring the mass of the shaft (with respect to that of the rotor), we have the following shaft distortion equations (Fig. 8):

$$y = \alpha_{11}\ m\ \omega^2\ y - \alpha_{11}\ P\ \beta - \alpha_{12}\ Y_d\ \omega\ \beta(2\Omega-\omega)$$

$$\beta = \alpha_{12}\ m\ \omega^2\ y - \alpha_{12}\ P\ \beta - \alpha_{22}\ Y_d\ \omega\ \beta(2\Omega-\omega)$$

we now find y/β from the first and second equation and equate the results, so that we have:

$$\frac{\alpha_{11} P + \alpha_{12}\ Y_d\ \omega(2\Omega-\omega)}{\alpha_{11}\ m\ \omega^2 - 1} = \frac{1 + \alpha_{12}\ P + \alpha_{22}\ Y_d\ \omega(2\Omega-\omega)}{\alpha_{12}\ m\ \omega^2}$$

By eliminating the denominators and arranging the terms in descending order of powers of ω, we obtain the expression:

$$\omega^4(-m\ \alpha_{11}\ \alpha_{22}\ Y_d + m\ \alpha_{12}^2\ Y_d) + \omega^3(m\ \alpha_{11}\ \alpha_{22}\ Y_d\ 2\Omega -$$

$$- m\alpha_{12}^2\ Y_d\ 2\Omega) + \omega^2(\alpha_{22}\ Y_d + m\alpha_{11}) + \omega(-\alpha_{22}\ Y_d\ 2\Omega) - (1 + \alpha_{12}\ P) = 0$$

which is the equation for the precession velocity.

This, it will be observed, is an algebraic equation of the fourth degree in ω, so that for a given shaft supporting at its end a given rotor and rotating at a certain velocity Ω, there are four characteristic precession velocities.

The system in question therefore has, for any Ω, four precession velocities which will now be calculated.

With reference to Fig. 5, the values to be introduced into the equation for the calculation of the precession velocities are:

$m = P/g \simeq 0.0306$ Kg sec^2/cm

$Y_d = Y_p/2 \simeq 1.405$ Kg cm sec^2

$E \simeq 2 \times 10^6$ Kg/cm^2 (modulus of elasticity of shaft material)

$J_1 \simeq 1.15$ cm^4 (moment of inertia of 22 mm diameter shaft-section)

$J_2 \simeq 0.0004$ cm^4 (moment of inertia of 3 mm diameter shaft-section)

$$\alpha_{11} = \frac{1}{3}\left(\frac{l_1^3}{E\,J_1} + \frac{l_2^3 - l_1^3}{E\,J_2}\right) \simeq 8.46 \text{ cm}$$

$$\alpha_{12} = \frac{(l_2 - l_1)^2}{2\,E\,J_2} + \frac{(l_2 - l_1)l_1}{E\,J_2} + \frac{l_1^2}{2\,E\,J_1} \simeq 0.352$$

$$\alpha_{22} = \frac{l_2 - l_1}{E\,J_2} + \frac{l_1}{E\,J_1} \simeq 0.015$$

On the basis of these values, the precession-velocity equation for our chopper-rotor is:

$$\omega^4 - 2\Omega\,\omega^3 - 2{,}150\,\omega^2 + 322\,\Omega\omega + 94{,}600 = 0$$

The numerical solution of this equation is time-consuming and it is therefore better to transform it into the following:

$$\Omega = \frac{\omega^4 - 2{,}150\,\omega^2 + 94{,}600}{2\,\omega^3 - 322\,\omega}$$

solving for Ω.

With this last equation it is easy to draw up the following table, by assigning various positive numerical values to ω and determining the corresponding values for Ω :

ω 1/sec	ω^2	ω^3	ω^4	$\omega^4 - 2{,}150\ \omega^2 +$ $+ 9.46 \times 10^4$	$2\ \omega^3 - 322\ \omega$	Ω 1/sec
1	1	1	1	9.245×10^4	-320	-289
2	4	8	16	8.601×10^4	-628	-137
3	9	27	81	7.533×10^4	-912	-82.6
4	16	64	256	6.045×10^4	-1.16×10^3	-52
5	25	125	625	4.152×10^4	-1.36×10^3	-30.5
6	36	216	1.3×10^3	1.850×10^4	-1.5×10^3	-12.3
7	49	343	2.4×10^3	-8×10^3	-1.568×10^3	5.1
8	64	512	4.1×10^3	-3.93×10^4	-1.552×10^3	25.4
9	81	729	6.56×10^3	-7.284×10^4	-1.44×10^3	50.6
10	100	10^3	10^4	-1.104×10^5	-1.22×10^3	90
11	121	1.33×10^3	1.47×10^4	-1.507×10^5	-880	171
12	144	1.73×10^3	2.07×10^4	-1.947×10^5	-400	487
13	169	2.2×10^3	2.85×10^4	-2.40×10^5	220	-1.09×10^3
14	196	2.74×10^3	3.84×10^4	-2.890×10^5	980	-295
15	225	3.38×10^3	5.06×10^4	-3.388×10^5	1.93×10^3	-175
20	400	8×10^3	1.6×10^5	-6.054×10^5	9.56×10^3	- 63.2
25	625	1.5×10^4	3.9×10^5	-8.554×10^5	2.196×10^4	- 39
30	900	2.7×10^4	8.1×10^5	-1.035×10^6	4.434×10^4	- 23.4
35	1.225×10^3	4.29×10^4	1.5×10^6	-1.045×10^6	7.4×10^4	- 14.2
40	1.6×10^3	6.4×10^4	2.56×10^6	-7.854×10^5	1.151×10^5	- 6.8
45	2.02×10^3	9.12×10^4	4.12×10^6	-1.254×10^5	1.679×10^5	- 0.745

ω 1/sec	ω^2	ω^2	ω^4	$\omega^4 - 2{,}150\ \omega^2 +$ $+ 9.46 \times 10^4$	$2\ \omega^3 - 322\ \omega$	Ω 1/sec
50	2.5×10^3	1.25×10^5	6.25×10^6	9.746×10^5	2.339×10^5	4.16
60	3.6×10^3	2.16×10^5	1.3×10^7	5.354×10^6	4.127×10^5	13
70	4.9×10^3	3.43×10^5	2.4×10^7	1.354×10^7	6.635×10^5	20.4
80	6.4×10^3	5.10×10^5	4.1×10^7	2.731×10^7	9.982×10^5	27.4
90	8.1×10^3	7.3×10^5	6.56×10^7	4.827×10^7	1.431×10^6	33.8
100	10^4	10^6	10^8	7.859×10^7	1.967×10^6	40
150	2.25×10^4	3.37×10^6	5.06×10^8	4.577×10^8	6.691×10^6	68.5
200	4×10^4	8×10^6	1.6×10^9	1.514×10^9	1.593×10^7	95
250	6.25×10^4	1.57×10^7	3.91×10^9	3.776×10^9	3.132×10^7	120
300	9×10^4	2.7×10^7	8.1×10^9	7.906×10^9	5.39×10^7	147
350	1.225×10^5	4.28×10^7	1.5×10^{10}	1.473×10^{10}	8.548×10^7	173
400	1.6×10^5	6.4×10^7	2.56×10^{10}	2.525×10^{10}	1.278×10^8	198
450	2.02×10^5	9.12×10^7	4.12×10^{10}	4.076×10^{10}	1.822×10^8	224
500	2.5×10^5	1.25×10^8	6.25×10^{10}	6.196×10^{10}	2.498×10^8	248
600	3.6×10^5	2.16×10^8	1.3×10^{11}	1.292×10^{11}	4.318×10^8	300
700	4.9×10^5	3.43×10^8	2.4×10^{11}	2.389×10^{11}	6.857×10^8	348
800	6.4×10^5	5.12×10^8	4.1×10^{11}	4.086×10^{11}	1.023×10^9	399
900	8.1×10^5	7.3×10^8	6.56×10^{11}	6.542×10^{11}	1.46×10^9	449
1000	10^6	10^9	10^{12}	9.978×10^{11}	1.999×10^9	500

For values of $\omega > 1{,}000$, $\Omega \simeq \omega/2$

The values in this table were calculated by slide-rule and rounded off.

Moreover, a simple study of the equation $\Omega = f(\omega)$ tells us that it has:

- three points of indetermination:

$$\omega = 0 \qquad \omega = 12.7 \qquad \omega = -12.7 \text{ rad/sec}$$

which are obtained when its denominator $2\omega^3 - 322\,\omega$ is equated with zero;

- four points of intersection with the axis ω :

$$\omega_{1.2} = \pm 46 \qquad \omega_{3.4} = \pm 6.63 \text{ rad/sec}$$

- for $\omega \to \pm \infty$ tends towards $\pm \infty$.

By plotting the values for ω in ordinates and the corresponding Ω values, calculated above, in abscissae, we obtained the variation law for the precession speeds of the chopper as a function of its rotational speed, as shown in Fig. 9.

The values of Ω for negative ω were not calculated, because it can be seen by checking that they are exactly symmetrical with the values calculated above, about the vertical ω axis.

3.3 Determination of the critical precession velocities

For the chopper we are considering, there are four possible precession velocities ω, which vary with the rotational velocity Ω according to the law represented in Fig. 9.

This law is symmetrical about the vertical ω axis, which means that the four precession velocities are independent of the direction of the chopper's rotation.

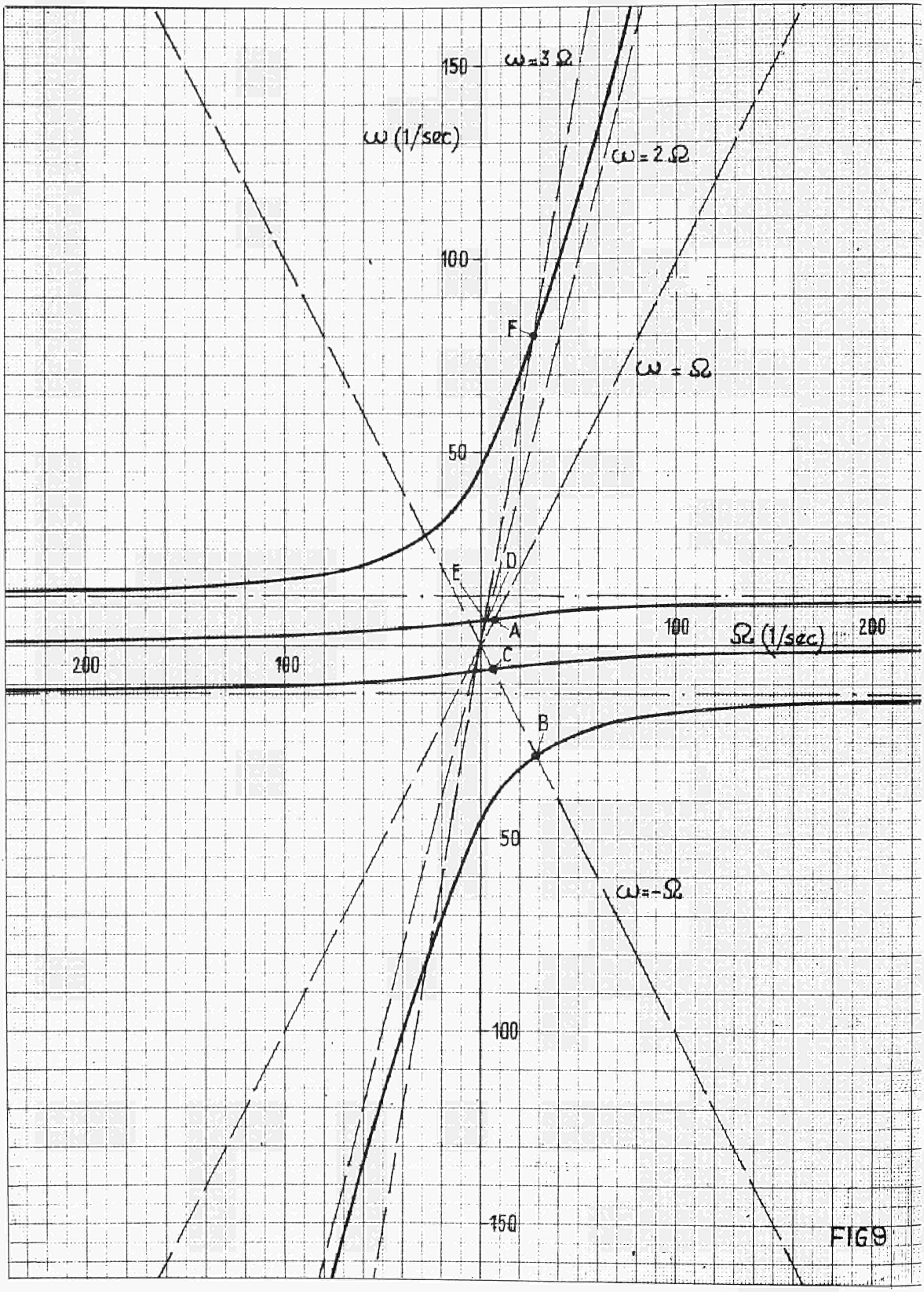

ω (1/sec)
150
100
50
50
100
150
ω = 3 Ω
ω = 2 Ω
ω = Ω
ω = -Ω
Ω (1/sec)
200
100
100
200
A
B
C
D
E
F

FIG9

According to Stodola (Ref. 7), critical conditions can occur in a rotating system where the ω/Ω ratio has the following values:

$$\frac{\omega}{\Omega} = 1; \quad -1; \quad +2 \text{ and } +3$$

We then plot on the graph in Fig.9 the dotted straight lines corresponding to these values of ω/Ω. They meet the precession-speed variation law at the points

A	the straight line $\omega/\Omega = +1$
B and C	the straight line $\omega/\Omega = -1$
D	the straight line $\omega/\Omega = +2$
E and F	the straight line $\omega/\Omega = +3$

At these points the rotational velocities Ω of the chopper are as follows:

point A	$\Omega_A = 7$ rad/sec	
points B and C	$\Omega_B = 29$ rad/sec	and $\Omega_C = 7$ rad/sec
point D	$\Omega_D = 3.5$ rad/sec	
points E and F	$\Omega_E = 2$ rad/sec	and $\Omega_F = 27$ rad/sec

which may thus be critical velocities for our system.

The corresponding rotational speeds are:

$n_A \simeq 67$ rpm ; $\quad n_B \simeq 280$ rpm ; $\quad n_C \simeq 67$ rpm

$n_D \simeq 33$ rpm ; $\quad n_E \simeq 19$ rpm ; $\quad n_F \simeq 260$ rpm

4. CONCLUSIONS

The chopper under study has the following critical velocities in the range 0 - 40,000 rpm:

- torsional ones in the range from 0 to about 5000 rpm, as given by equation (6) of section 1.3.2
- two flexional, at 64 rpm and 29,500 rpm
- five precessional, at 19 rpm; 33 rpm; 67 rpm; 260 rpm; 280 rpm.

The operating speed

$n \simeq 22{,}000$ rpm

arrived at in the report "Calculation of Chopper Rotor Centrifugal Stresses" (8), can be regarded as sufficiently distant from these for a well-balanced system and in theory, therefore, should ensure satisfactory operation of the chopper.

The chopper shaft dimensions shown in Fig. 4, which give rise to the foregoing critical velocities for the attached rotor, were not chosen haphazardly; they are the outcome of a study of the three above-named types of critical velocity.

Calculations on various systems, obtained by varying the shaft dimensions but keeping to the overall length dictated by practical reasons, showed that the dimensions of the small-diameter (5 mm) shaft-section have a proponderant influence on the critical velocities of the system, and principally on the flexional critical velocities.

Specifically, if we keep the diameter of the narrow shaft-section unchanged, for the reason given in the introduction, but vary its length so that the section (22 mm diameter) immediately above the rotor (Fig. 4) varies and the other lengths remain constant, the critical torsional velocities,

DIAGRAM OF THE SECOND CRITICAL VELOCITY AS FUNCTION OF THE LENGTH l_2 (L AND l_1 CONST., l_3 VARIABLE)

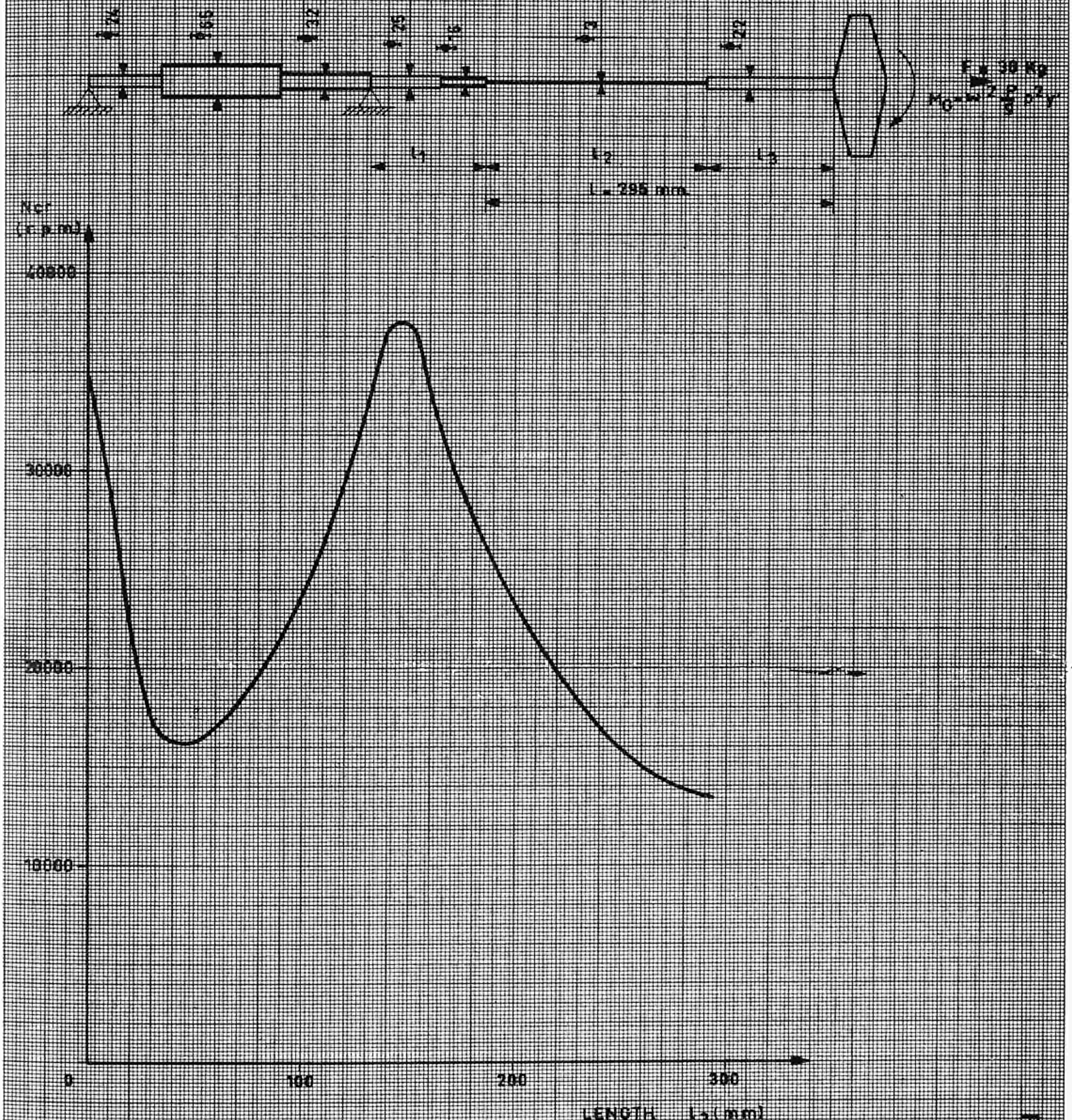

FIG. 10

the first critical flexional velocity and the critical velocities due to precession differ by little from the values calculated above (at any rate within a certain range of narrow shaft-length) while the second critical flexional velocity varies widely.

The law governing the variation of the last-named with the varying length of the narrow shaft as described above is shown in Fig. 10. Bearing in mind the purpose of the narrow shaft-section, and noting that it is better fulfilled as this section is lengthened, we can see from the graph in Fig.10 that the optimum length, offering the highest degree of safety in respect of the second critical flexional velocity, is 145 - 150 mm.

Practical considerations prevented our adopting this length, so we chose the nearest possible length, namely 120 mm, on which the calculations in the present report are based.

5. EXPERIMENTAL RESULTS

The system under consideration was constructed. Fig. 11 shows the finished device. It has been equipped with two different lengths, 100 mm and 120 mm, of narrow shaft 3 mm in diameter: tests were carried out on both and are described below.

5.1 Test with small diameter shaft of length 100 mm

This was the first of the test performed. The system showed an instability in the range of asynchronous operation (0 - about 5000 rpm) characterized by transversal and torsional vibrations. These were observed through a plexi-glass blank flange which can be seen on Fig.11, by means of a telescope and by simultaneously displaying the pulses of a magnetic pick-up and a photoelectric cell on the screen of an oscilloscope. The pick-up is mounted above, the cell below the narrow shaft.

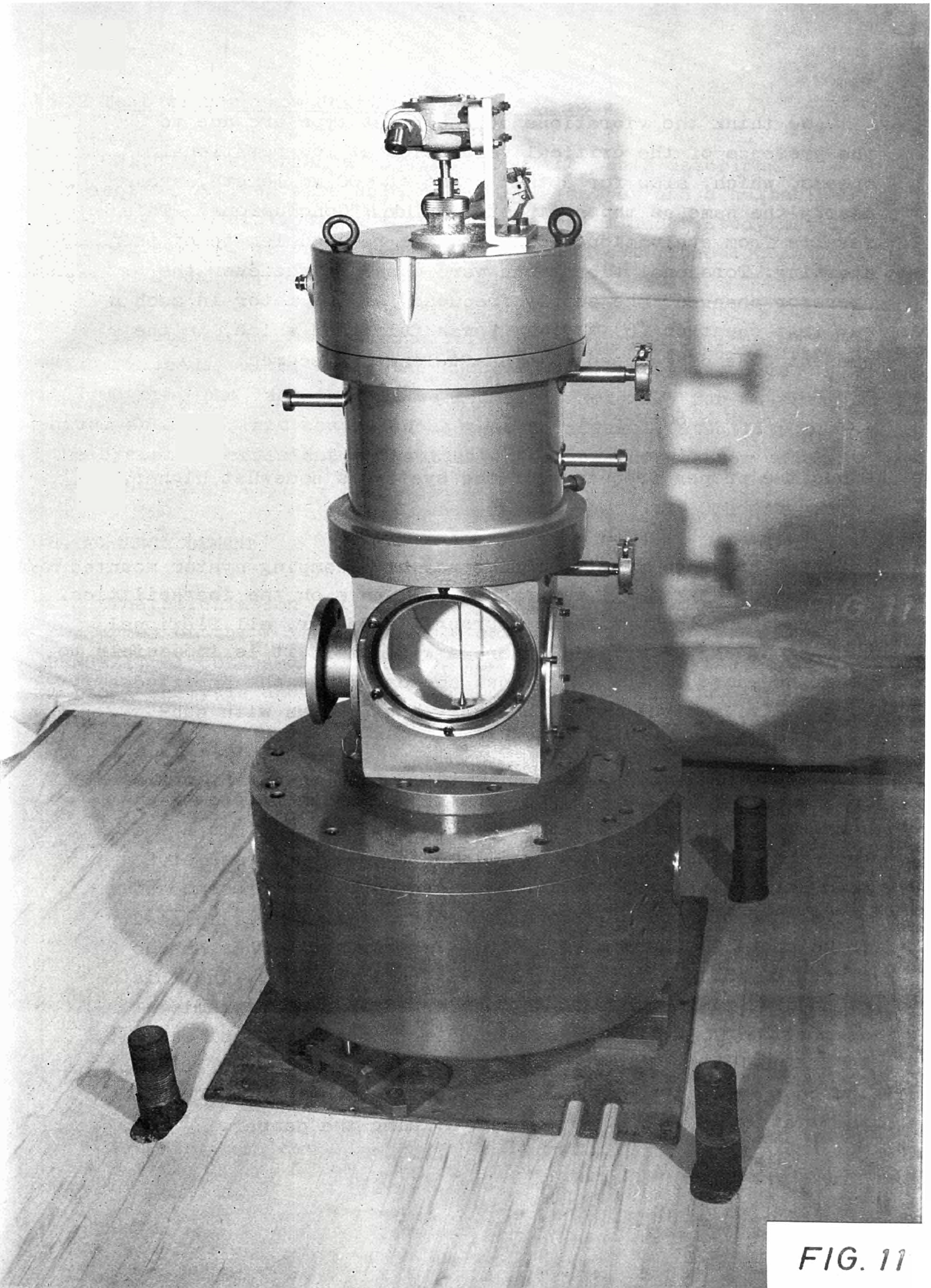

FIG. 11

We think the vibrations of the first type are due to the presence of the critical velocities at low rotational speeds, which, also for a thin shaft of 100 mm length, are nearly the same as those given in section 4 "Conclusions" This results from evaluations done with the reduced length of thin shafting. Torsional vibrations were observed whenever the operator changed the supply frequency of the motor in such a way that equation (8) of section 1 was fulfilled which, in the present case of reduced thin shaft length, becomes:

$$N = 60\ F - 415$$

since the proper frequency of the system is somewhat higher, namely $f \simeq 830$ rpm.

The presence and the efficiency of a damping system mounted below the chopper disk has a remarkable influence on the instabilities. It turned out that, with an appropriate damper, all flexional vibrations can be avoided, whereas without it it is impossible to pass the range of low rotational speeds, since the amplitudes of these vibrations reach then very high values with subsequent failure of the thin shaft.

With the damper, beyond about 5000 rpm the system was completely steady up to about 23,000 rpm. Around this speed the narrow shaft began to oscillate transversally and at 23,500 rpm it failed; failure was caused by the presence of the second critical flexional velocity, which is calculated to be about 23,800 rpm (Fig. 10). Clearly the damper has no effect on this second critical flexional velocity, and this is understandable when it is considered that the dynamic distortion of the shaft associated with this critical velocity is of such a configuration that during vibration the rotor of the chopper is transversally montionless, just as the stub-shaft attached to its bottom and holding the damper.

5.2 Test with narrow shaft of length 120 mm

With the experience acquired from the tests described in section 4.1, we were able to devise a damper and a suitable starting acceleration, so that the new system under study was demonstrated to be free from even the slightest vibration between 0 and 25,000 rpm.

Practical and safety considerations deterred us from higher speeds; also, since the chopper's operating speed is 22,000 rpm, the fact that it worked satisfactorily for several hours at 25,000 rpm convinced us that the dynamic stability of the system is efficient and suitable for the purpose for which it was designed.

6. ACKNOWLEDGEMENT

The calculation of critical flexional velocities has been performed on the "CETIS" IBM 7090 computer. I thank Messrs. BENUZZI, DI COLA and MONTEROSSO, who contributed to the mathematical analysis and carried out the program on computer.

I also wish to thank Mr. HEINZ GEIST to whom I am indebted for his valuable advice and suggestions.

APPENDIX I

In section 2, which dealt with the "Calculation of **critical flexional velocities",** the classical theory (4),(5),(11),(12) of the flexional vibrations of the beams was used, so that the effects of rotatory inertia and the effect of transverse shear on the **critical flexional velocities were disregarded. It is known** (12,(13) (see also the table at the end of this Appendix) that the percentage errors introduced by failure to take these effects into account are insignificant when the dimensions of the cross-section are small in relation to the length of the shaft, and when only the first two critical speeds are considered; this is in fact the case in the present instance.

When the above conditions are no longer satisfied (cross-section not small in relation to length, and critical velocities higher than the second considered), the effects mentioned must be taken into account in order to avoid errors of more than 40% in the determination of the critical speed (13).

In this case one obtains the following Timoshenko equation (11, (12), which is valid for any uniformly loaded length of shaft of constant cross-section and held only at its extremities, this equation being subject to the limiting conditions for the length in question:

$$EJ\,\frac{\delta^4 y}{\delta x^4} + \frac{\gamma S}{g}\,\frac{\delta^2 y}{\delta t^2} - \left(\frac{\gamma J}{g} + \frac{EJ\gamma}{gK'G}\right)\frac{\delta^4 y}{\delta x^2\,\delta t^2} + \frac{\gamma^2 J}{g^2 K' G}\,\frac{\delta^4 y}{\delta t^4} = 0$$

where G = modulus of transverse elasticity

K' = coefficient of shear deformability, which can vary with the shape of the cross-section (3).

If we consider only the stationary vibrations (4), the solution is of the type:

$$y(x,t) = f(x).f(t)$$

In particular, since the motion is harmonic (4), the factor f(t) is of the type sin Ωt, so that:

$$y(x,t) = f(x).\sin \Omega t$$

By substituting of the derivatives d^4y/dx^4, d^2y/dt^2, d^4y/dx^2dt^2, and d^4y/dt^4 in the Timoshenko equation, we obtain:

$$EJf^{IV}(x)\sin \Omega t - \frac{\gamma S}{g}\,\Omega^2 f(x)\sin \Omega t + \left(\frac{\gamma J}{g} + \frac{EJ\gamma}{gK'G}\right)\Omega^2 f''(x)\sin \Omega t +$$

$$+ \frac{\gamma^2 J}{g^2 K'G}\,\Omega'' f(x)\sin \Omega t = 0$$

i.e.

$$f^{IV}(x) + \left(\frac{\gamma\Omega^2}{Eg} + \frac{\gamma\Omega^2}{gK'G}\right) \qquad f''(x) + \left(\frac{\gamma^2\Omega^4}{Eg^2K'G} - \frac{\gamma S\Omega^2}{EJg}\right) f(x) = 0$$

If the revolving shaft is subjected to an axial tensile or compressive force F, the term $-F/EJ\ f''(x)$ (where F is positive for a tensile force) (4) is added to the left-hand side, and the equation becomes:

$$f^{IV}(x) + \left(\frac{\gamma\Omega^2}{Eg} + \frac{\gamma\Omega^2}{gK'G} - \frac{F}{EJ}\right) f''(x) + \left(\frac{\gamma^2\Omega^4}{Eg^2K'G} - \frac{\gamma S\Omega^2}{EJg}\right) f(x) = 0 \qquad (28)$$

This equation is of the same type as (25) so that by means of the method of calculation described in **section 2 of the present** report, it is possible to determine the **critical flexional velocities** taking into account all the effects mentioned above.

The following table shows the critical **velocities of the** system of Fig. 4, as found from formulae (25) and (28).

Order of critical **velocities**	Values of the critical **velocities** (r.p.m.)	
	Formula (25)	Formula (28)
1	~ 64	~ 64
2	~ 29,500	~ 29,500
3	~ 58,000	~ 58,000
4	~ 70,000	~ 69,000

APPENDIX II

The critical flexional velocities can also be calculated by the approximate method described by Myklestad [14] and later improved by T.C. Huang and N.C. Wu [13].

The results obtained by this method are very close [13] to the values obtained for the critical velocities from the Timoshenko equation, even for high orders of critical velocities.

REFERENCES

1. G.ROSSI "Il calcolo delle vibrazioni torsionali nei motori a combustione interna" Collana tecnica "Fiat - Grandi motori", 1944

2. W. KER WILSON "Practical solution of torsional vibration problems" Vol. I and II - CHAPMAN & HALL LTD, LONDON, 1956 - 1963

3. Odone BELLUZZI "Scienza delle costruzioni", Vol. I, Bologna (Nicola Zanichelli Editore), 1953

4. Odone BELLUZZI "Scienza delle costruzioni", Vol. IV, Chap. XXXIV : Le vibrazioni, Bologna (Nicola Zanichelli Editore), 1955

5. P.E. BRUNELLI "Le velocità critiche degli alberi", Naples (R. Ponti), 1921

6. B. FINZI "Meccanica razionale", Nicola Zanichelli, Bologna, 1959

7. J.P. DEN HARTOG "Vibrationsmécaniques", Dunod, Paris, 1960

8. M. BIGGIO and H. GEIST "Calculation of Chopper Rotor centrifugal Stresses" Report Euratom, to be published

9. C.B. BIENZENO and R. GRAMMEL "Technische Dynamik", Berlin:Göttingen Heidelberg (Publisher: Springer), 1953

10. J.W.S. RAYLEIGH "The theory of sound", Dover Publications, New York, 1945

11. Lydik S. Jacobsen and R.S. AYRE "Engineering Vibrations" McGRAW-HILL, Book Company Inc., New York, 1958

12. S. TIMOSHENKO "Théorie des vibrations" Paris et Liège, Librairie Polytechnique Ch. Béranger, Paris, 1954

13. T.C. HUANG and N.C. WU "Approximate analysis of flexural vibrations of beams" - "Developments in mechanics" Vol. 1, Edited by J.E. LAY and L.E. Malvern, 1961

14. N.O. MYKLESTAD "A new method of calculating natural modes of uncoupled bending vibration of airplane wings and other types of beams" J. of Aeronautical Sciences, Nr. 2,1944 pp. 153-162

NOTICE TO THE READER

All Euratom reports are announced, as and when they are issued, in the monthly periodical **EURATOM INFORMATION**, edited by the Centre for Information and Documentation (CID). For subscription (1 year: US$ 15, £ 5.7) or free specimen copies please write to:

Handelsblatt GmbH
"Euratom Information"
Postfach 1102
D-4 Düsseldorf (Germany)

or

Office central de vente des publications
des Communautés européennes
2, Place de Metz
Luxembourg

To disseminate knowledge is to disseminate prosperity — I mean general prosperity and not individual riches — and with prosperity disappears the greater part of the evil which is our heritage from darker times.

Alfred Nobel

SALES OFFICES

All Euratom reports are on sale at the offices listed below, at the prices given on the back of the front cover (when ordering, specify clearly the EUR number and the title of the report, which are shown on the front cover).

OFFICE CENTRAL DE VENTE DES PUBLICATIONS DES COMMUNAUTES EUROPEENNES
2, place de Metz, Luxembourg (Compte chèque postal N° 191-90)

BELGIQUE — BELGIË
MONITEUR BELGE
40-42, rue de Louvain - Bruxelles
BELGISCH STAATSBLAD
Leuvenseweg 40-42 - Brussel

DEUTSCHLAND
BUNDESANZEIGER
Postfach - Köln 1

FRANCE
SERVICE DE VENTE EN FRANCE DES PUBLICATIONS DES COMMUNAUTES EUROPEENNES
26, rue Desaix - Paris 15e

ITALIA
LIBRERIA DELLO STATO
Piazza G. Verdi, 10 - Roma

LUXEMBOURG
OFFICE CENTRAL DE VENTE DES PUBLICATIONS DES COMMUNAUTES EUROPEENNES
9, rue Goethe - Luxembourg

NEDERLAND
STAATSDRUKKERIJ
Christoffel Plantijnstraat - Den Haag

UNITED KINGDOM
H. M. STATIONERY OFFICE
P. O. Box 569 - London S.E.1

EURATOM — C.I.D.
51-53, rue Belliard
Bruxelles (Belgique)